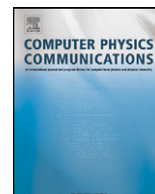




Contents lists available at ScienceDirect

## Computer Physics Communications

www.elsevier.com/locate/cpc

An open-source library for the numerical modeling of mass-transfer in solid oxide fuel cells<sup>☆</sup>Valerio Novaresio<sup>a,1</sup>, María García-Camprubí<sup>b,1</sup>, Salvador Izquierdo<sup>a,2</sup>, Pietro Asinari<sup>a,\*</sup>, Norberto Fueyo<sup>b</sup><sup>a</sup> Dipartimento di Energetica, Politecnico di Torino, Corso Duca degli Abruzzi 24, 1019, Torino, Italy<sup>b</sup> Área de Mecánica de Fluidos-LITEC, Universidad de Zaragoza, María de Luna 3, 50018, Zaragoza, Spain

## ARTICLE INFO

## Article history:

Received 14 January 2011

Received in revised form 4 August 2011

Accepted 5 August 2011

Available online xxxx

## Keywords:

Solid oxide fuel cell

Multicomponent

Mass-transfer

Porous media

OpenFoam®

## ABSTRACT

The generation of direct current electricity using solid oxide fuel cells (SOFCs) involves several interplaying transport phenomena. Their simulation is crucial for the design and optimization of reliable and competitive equipment, and for the eventual market deployment of this technology. An open-source library for the computational modeling of mass-transport phenomena in SOFCs is presented in this article. It includes several multicomponent mass-transport models (*i.e.* Fickian, Stefan–Maxwell and Dusty Gas Model), which can be applied both within porous media and in porosity-free domains, and several diffusivity models for gases. The library has been developed for its use with OpenFOAM®, a widespread open-source code for fluid and continuum mechanics. The library can be used to model any fluid flow configuration involving multicomponent transport phenomena and it is validated in this paper against the analytical solution of one-dimensional test cases. In addition, it is applied for the simulation of a real SOFC and further validated using experimental data.

## Program summary

Program title: multiSpeciesTransportModels

Catalogue identifier: AEKB\_v1\_0

Program summary URL: [http://cpc.cs.qub.ac.uk/summaries/AEKB\\_v1\\_0.html](http://cpc.cs.qub.ac.uk/summaries/AEKB_v1_0.html)

Program obtainable from: CPC Program Library, Queen's University, Belfast, N. Ireland

Licensing provisions: GNU General Public License

No. of lines in distributed program, including test data, etc.: 18 140

No. of bytes in distributed program, including test data, etc.: 64 285

Distribution format: tar.gz

Programming language: C++

Computer: Any x86 (the instructions reported in the paper consider only the 64 bit case for the sake of simplicity)

Operating system: Generic Linux (the instructions reported in the paper consider only the open-source Ubuntu distribution for the sake of simplicity)

Classification: 12

External routines: OpenFOAM® (version 1.6-ext) (<http://www.extend-project.de>)

**Nature of problem:** This software provides a library of models for the simulation of the steady state mass and momentum transport in a multi-species gas mixture, possibly in a porous medium. The software is particularly designed to be used as the mass-transport library for the modeling of solid oxide fuel cells (SOFC). When supplemented with other sub-models, such as thermal and charge-transport ones, it allows the prediction of the cell polarization curve and hence the cell performance.

**Solution method:** Standard finite volume method (FVM) is used for solving all the conservation equations. The pressure-velocity coupling is solved using the SIMPLE algorithm (possibly adding a porous drag term if required). The mass transport can be calculated using different alternative models, namely Fick,

<sup>☆</sup> This paper and its associated computer program are available via the Computer Physics Communications homepage on ScienceDirect (<http://www.sciencedirect.com/science/journal/00104655>).

\* Corresponding author. Tel.: +39 011 090 4520.

E-mail address: [pietro.asinari@polito.it](mailto:pietro.asinari@polito.it) (P. Asinari).

<sup>1</sup> These authors contributed equally to this work.

<sup>2</sup> Current affiliation: Instituto Tecnológico de Aragón (ITA), María de Luna 8, 50018 Zaragoza, Spain.

Maxwell–Stefan or dusty gas model. The code adopts a segregated method to solve the resulting linear system of equations. The different regions of the SOFC, namely gas channels, electrodes and electrolyte, are solved independently, and coupled through boundary conditions.

*Restrictions:* When extremely large species fluxes are considered, current implementation of the Neumann and Robin boundary conditions do not avoid negative values of molar and/or mass fractions, which finally end up with numerical instability. However this never happened in the documented runs. Eventually these boundary conditions could be reformulated to become more robust.

*Running time:* From seconds to hours depending on the mesh size and number of species. For example, on a 64 bit machine with Intel Core Duo T8300 and 3 GBytes of RAM, the provided test run requires less than 1 second.

© 2011 Elsevier B.V. All rights reserved.

## 1. Introduction

Overall energy use is closely linked to population and economic growth. The latest projections imply that total world consumption of energy will increase at an average annual rate of 1.5% from 2007 to 2030 [1]. Environmental concerns associated to the conventional (thermal) generating technologies, such as global warming, underpin the need of finding cleaner energy sources. As a result, some partial alternatives are emerging, including the use of fuel cells [2].

Fuel cells offer the potential of reducing the environmental impact and, to some extent, the energy dependency associated to the use of fossil fuels. A fuel cell is an electrochemical device that converts the chemical energy of a fuel directly into electrical energy and heat, offering higher efficiency, lower emissions and lower noise pollution than conventional technologies. In the last years, the research effort has mainly focused on two types of fuel cell: the polymer electrolyte fuel cell (PEMFC) and the solid oxide fuel cell (SOFC) [3]. The latter is the aim of the present work.

The term SOFC usually refers to a solid oxide fuel cell stack, a high temperature device composed of several single units or cells. A single unit of a SOFC consists of: a solid electrolyte, two porous electrodes, a fuel channel, an oxidant channel and the electrical interconnects. The operating principle of a single cell, depicted in Fig. 1, involves several intertwined phenomena. As shown in Fig. 1, air flows along the air channel and through the cathode until it reaches the cathode–electrolyte interface, where it is reduced to oxygen anions by the electrons present in the cathode. The oxygen anions cross the electrolyte to the electrolyte–anode interface. On the other side of the electrolyte, the fuel flows along the fuel channel and through the anode until it reaches the anode–electrolyte interface, where it is oxidized. At the same time, reaction products flow away from this region through the porous anode to the channel, where they are convected to the outlet. The electrons involved in the oxidation reaction flow into the anode, and then move from the anode to the cathode producing direct-current electricity in the external circuit. A deeper insight into the SOFC technology including component requirements, material properties, cell geometries, stack configurations, fuel flexibility, mobile and stationary applications, limitations and ongoing research goals can be found in several sources in the literature [2–6].

Although there are some pre-commercial SOFC prototypes [7–10], some remaining challenges need to be overcome before their wider commercial availability. In recent years, much of the SOFC development has been directed to the search for new materials, to improve the power density and to reduce the operating temperature. However, most of the parameters that affect the cell performance, such as the species, current density and temperature distributions, are difficult to acquire experimentally. Thus, SOFC developers look for the help of modeling tools to gain a fuller understanding of the experimental evidence [11].

Andersson et al. (2010) [12] have recently conducted a thorough review of the state of the art in SOFC modeling. Their report points out the multiphysics and multiscale nature of a SOFC, where mass, heat, momentum and charge transport take place simultaneously due to a microcatalytic electrochemical reaction. Their work also shows a wide agreement about the fundamental equations that describe momentum transport (Navier–Stokes, Darcy's Law) and charge transport (Ohm's Law). However, the description of the mass and heat transfer mechanisms is not straightforward.

Regarding mass transfer, three distinct mechanisms are present in a SOFC: convection, molecular diffusion and Knudsen diffusion; the latter is relevant only in the electrodes, where depending on the values of the porosity parameters ( $d_p$ ,  $\tau$ ,  $\varepsilon$ ,  $B_0$ ), one of these mass-transfer mechanisms may govern the overall mass-transfer process and the rest may become negligible. Moreover, molecular diffusion in the cathode is usually binary (since the oxidant is air, made up of  $O_2$  and  $N_2$ ), while in the anode it may be binary or multicomponent, depending on the fuel mixture (for pure  $H_2$ , the mixture is  $H_2 + H_2O$ ; for hydrocarbons, it is  $C_xH_y + H_2 + H_2O + CO + CO_2$ ). Thus, depending on the cell materials and operating conditions, different mass-transfer models are applicable. As a consequence, there is a wide range of models to describe the mass-transfer in a SOFC. Some authors consider all three mechanism [13–17], while other authors neglect the convective mass flow in the electrodes [18–21]. With regard to the diffusion constitutive equation, some authors use Fick's for both binary and multicomponent molecular diffusion, either in the channels or in the porous media, using an effective diffusion coefficient [22, 23]. On the other hand, Stefan–Maxwell equations for multicomponent ordinary diffusion are used in [13,16] for the channel; while for the porous media a modified Stefan–Maxwell model, including Knudsen effects, is employed in [19]. Moreover, the Dusty Gas Model [24] is preferred in [13,17] to model the global mass transfer in the electrodes, despite its increased complexity, because its higher accuracy [20].

Much of the published studies featuring SOFC modeling use three commercial codes: FLUENT® [25,26], Star-CD® [23,27,28] and COMSOL Multiphysics® [15,16,29]; there are also some academic and in-house codes [13,17,22] only available to the corresponding developers. However, there is not as yet an open-source code for SOFC modeling. For those SOFC researchers lacking advanced programming skills (or indeed time), the leeway for numerical simulations is limited to the options provided in commercial codes; and so is the choice of the mass-transfer models.

The aim of the present work is to implement a comprehensive mass-transfer library for multicomponent mixtures possibly flowing in a porous media. The library is particular conceived as, but not restricted to, a component for the modeling of SOFCs. The results have been

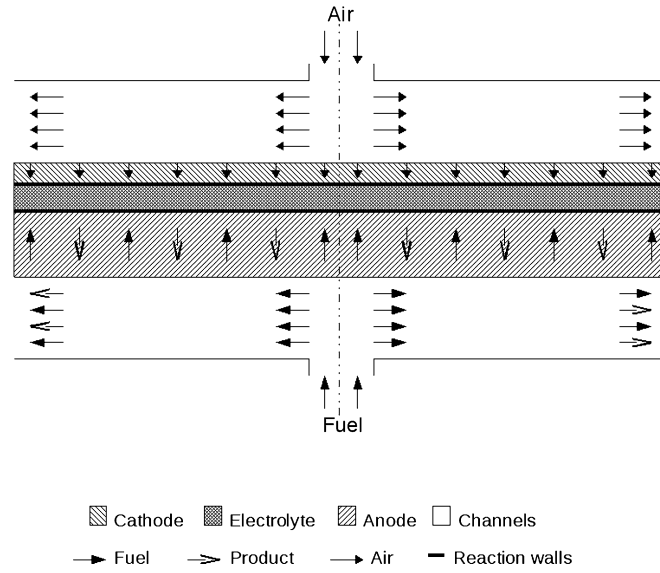


**Fig. 1.** Schematic of a circular-shaped planar solid oxide fuel cell.

validated against analytical solutions for simple mass-transfer problems, but also using experimental, gathered in the laboratory of some of the present authors, for an actual SOFC configuration.

The library is written in C++, can be run in parallel, and is compatible with the OpenFOAM® CFD Toolbox. The OpenFOAM® (Open Field Operation and Manipulation) CFD Toolbox is a free, open-source CFD software package. It has a large user base across many areas of Engineering and Science, in both commercial and academic organizations [30,31]. In this paper, the authors present the models contained in the library, their implementation in a structured set of efficient C++ modules and the corresponding validation.

## 2. Theoretical background: mass-transfer modeling for SOFCs

The global mass-transfer process in a solid oxide fuel cell takes place in three different media: (i) the channels; (ii) the electrodes; and (iii) the electrolyte.

This work addresses the modeling of molecular mass-transfer phenomena within the gases in the channels and electrodes; the transfer of charges in the solid electrolyte is therefore out of the scope of the library, but it can be tackled in a variety of ways; a simple one for thin electrolyte layers is used in the SOFC model presented below.

The equations governing mass-transfer phenomena stem from the application, to the given gases, of two basic laws of Mechanics: (i) the second law of Newton; and (ii) the mass-conservation principle. The corresponding equations are: the momentum-conservation equation and the continuity equation, which for reacting mixtures is extended to the chemical-species conservation equations.

### 2.1. Momentum-conservation equation

The momentum-conservation equation of the gas flowing in the channel is, in vector form:

$$\frac{\partial(\rho \vec{v})}{\partial t} + \nabla \cdot (\rho \vec{v} \vec{v}) - \nabla \cdot \vec{\tau}' = -\nabla p \quad (1)$$

where  $\rho$  is the fluid density,  $\vec{v}$  is the fluid mass-averaged velocity,  $\vec{\tau}'$  is the viscous stress tensor and  $p$  is the pressure. In the electrode domain, considering a porous medium with non-constant porosity ( $\varepsilon$ ), the momentum conservation equation of the gas is obtained after applying twice the spatial average theorem to Eq. (1) and considering some proper physical scalings for the spatial gradients (see [32] and references therein):

$$\begin{aligned} \varepsilon^{-1} \frac{\partial(\rho \langle \vec{v} \rangle)}{\partial t} + \varepsilon^{-1} \nabla \cdot (\varepsilon^{-1} \rho \langle \vec{v} \rangle \langle \vec{v} \rangle) - \nabla \cdot (\varepsilon^{-1} \langle \vec{\tau}' \rangle) \\ = -\nabla p - \mu \varepsilon^{-1} \nabla \varepsilon \cdot \nabla (\varepsilon^{-1} \langle \vec{v} \rangle) - \mu \vec{B}_0^{-1} \cdot \langle \vec{v} \rangle - \mu \vec{B}_0^{-1} \cdot \vec{F} \cdot \langle \vec{v} \rangle \end{aligned} \quad (2)$$

where  $\mu$  is fluid viscosity,  $\vec{B}_0$  is the porous-medium permeability-tensor,  $\vec{F}$  is the porous inertia tensor, and  $\langle \vec{v} \rangle = \varepsilon \vec{v}$  represents the superficial permeation velocity of the fluid through the porous media. Eq. (2) can be reduced, assuming steady state, Stokes flow, constant and isotropic porosity and negligible viscous effects, to Darcy's Law:

$$\langle \vec{v} \rangle = -\frac{B_0}{\mu} \nabla p \quad (3)$$

where  $B_0$  is a constant porous-medium permeability-coefficient.

**Table 1**  
Summary of the diffusion models in the mass-transfer library.

Clear, non-porous domains		Diffusion	Usage restricted to
Model	Eq.		
Fick	(10)	Ordinary	Binary mixtures
Fickian (I)	(13)	Ordinary	Highly convective flows
SM	(31)	Ordinary	
Porous domains		Phenomena	Usage restricted to
Model	Eq.		
Fickian (II)	(18)	Ordinary and Knudsen diffusion	Highly permeable media
DGM	(39)	Ordinary and Knudsen diffusion with viscous flow	

## 2.2. Mass-conservation equation

The continuity equation for a gas with non-constant density is:

$$\frac{\partial \rho}{\partial t} + \nabla \cdot (\rho \vec{v}) = S_y \quad (4)$$

where  $\vec{v}$  is given by Eq. (1) and  $S_y$  stands for the volumetric mass sources or sinks. In a porous medium with constant porosity, Eq. (4) the proper formulation of the continuity equation involves the medium porosity in the local accumulation term (to reflect that not all of the local space is available to the fluid) and the permeation velocity (which is different from the superficial velocity):

$$\frac{\partial(\varepsilon \rho)}{\partial t} + \nabla \cdot (\rho \langle \vec{v} \rangle) = S_y \quad (5)$$

where  $\varepsilon$  is the porosity of the porous matrix and  $\langle \vec{v} \rangle$  stands for the permeation velocity, Eq. (3).

## 2.3. Chemical-species equation

The equation for the conservation of the chemical species  $\alpha$  in the channels is written as:

$$\frac{\partial(\rho y_\alpha)}{\partial t} + \nabla \cdot (\rho y_\alpha \vec{v}) + \nabla \cdot \vec{j}_\alpha = S_{y_\alpha} \quad (6)$$

where  $\rho$  is the fluid density (Eq. (4)),  $\vec{v}$  is the fluid velocity (Eq. (1)),  $y_\alpha$  is the mass fraction of species  $\alpha$ ,  $\vec{j}_\alpha$  is the mass diffusion-flux of species  $\alpha$  relative to the mass-average velocity, and  $S_{y_\alpha}$  stands for the volumetric sources or sinks of the species  $\alpha$ . For the gas flowing through the electrodes, considering constant porosity, the chemical-species conservation equation is as follows:

$$\frac{\partial(\varepsilon \rho y_\alpha)}{\partial t} + \nabla \cdot (\rho y_\alpha \langle \vec{v} \rangle) + \nabla \cdot \vec{j}_\alpha = S_{y_\alpha} \quad (7)$$

In the previous equation, the flux  $\vec{j}_\alpha$  is defined per unit of physical area and the source term  $S_{y_\alpha}$  per unit of physical volume. We thus use the commonplace formalism in writing the previous equation for consistency with existing literature (in particular, for fuel cells modeling), where the effects of porosity are taken into account by the closure models for expressing the fluxes and the source terms.

The modeling of the diffusion flux ( $\vec{j}_\alpha$ ), either in Eq. (6) or in Eq. (7), depends on the medium where the diffusion is taking place (i.e. channel or porous medium), the nature of the gas (i.e. binary or multicomponent mixture) and the diffusion mechanisms taken into account (i.e. binary diffusion, Knudsen diffusion or both). In Section 2.4 the most common constitutive equations to model the diffusion fluxes in a SOFC are presented.

## 2.4. Diffusion-flux modeling

Diffusion plays an important role in the SOFC global mass transfer because convection is hindered in the electrodes, and hence mass-transfer becomes the limiting mass-transfer mechanism for the cell performance. Hence, to improve the overall accuracy of the SOFC model, the diffusion model must be carefully chosen. The mass-transport library presented in this work provides a survey of the diffusion models applicable to a SOFC: Fick and Stefan–Maxwell models for the gas diffusion in the porosity-free domains (channels); and Fick and dusty-gas models for the gas diffusion in porous media (electrodes). These models are described below, and summarized in Table 1.

### 2.4.1. Fick's model

In 1855, Fick postulated the fundamental law of ordinary diffusion by means of analogies with Fourier's work on thermal conduction [33–35]. He defined the 1D diffusion flow of a species  $\alpha$  in a species  $\beta$  in an isothermal and isobaric system as:

$$J_\alpha = -\mathcal{D}_{\alpha\beta} \frac{\partial c_\alpha}{\partial x} \quad (8)$$

where  $J_\alpha$  is the molar ordinary diffusion flux of species  $\alpha$  relative a molar-average velocity,  $\mathcal{D}_{\alpha\beta}$  is the diffusion coefficient and  $c_\alpha$  is the molar density of the species  $\alpha$ . A more general flux relation which is not restricted to isothermal, isobaric systems was proposed by Groot [36]:

$$\vec{J}_\alpha = -c \mathcal{D}_{\alpha\beta} \nabla x_\alpha \quad (9)$$

where  $c$  is the molar density of the gas mixture and  $x_\alpha$  is the molar fraction of species  $\alpha$ . Eq. (8) is a special form of Eq. (9), since for an ideal gas ( $c = p/RT$ ) the total concentration is constant under isothermal and isobaric conditions. A further equivalent expression, for the mass-diffusion flux relative to the mass average velocity, is [35,37]:

$$\vec{j}_\alpha = -\rho \mathcal{D}_{\alpha\beta} \nabla y_\alpha \quad (10)$$

Eqs. (8), (9) and (10) involve the same phenomenological binary diffusion coefficient, for which empirical correlations are given in Section 2.5. Substituting Eq. (10) into Eq. (6), we have:

$$\frac{\partial(\rho y_\alpha)}{\partial t} + \nabla \cdot (\rho y_\alpha \vec{v}) - \nabla \cdot (\rho \mathcal{D}_{\alpha\beta} \nabla y_\alpha) = S_{y_\alpha} \quad (11)$$

which is the mass-conservation equation of a species  $\alpha$  in a binary mixture. The mass-transfer of a binary mixture flowing through a channel is described by the set of equations given by Eq. (11) applied to all the species of the mixture but one, together with the momentum and continuity equations, Eqs. (1) and (4).

Partly because its simplicity makes it an attractive option, Fick's law has been extended in the SOFC literature to model also ordinary diffusion of multicomponent mixtures in the channels (Fickian (I)), and to model simultaneously ordinary and Knudsen diffusion in the electrodes (Fickian (II)) [22,23,38]. Both approximations are detailed below.

The diffusion coefficient of a species  $\alpha$  in a multicomponent gas system ( $\mathcal{D}_{\alpha m}$ ) is given by:

$$\mathcal{D}_{\alpha m} = \frac{1 - x_\alpha}{\sum_{\beta \neq \alpha} \left( \frac{x_\beta}{\mathcal{D}_{\alpha\beta}} \right)} \quad (12)$$

Eq. (12) stems from the Stefan–Maxwell equations [39] and was experimentally verified by Fairbanks and Wilke [40]. From Eqs. (10) and (12), the Fickian law for the ordinary diffusion flux of the species  $\alpha$  in a multicomponent mixture is:

$$\vec{j}_\alpha = -\rho \mathcal{D}_{\alpha m} \nabla y_\alpha \quad (13)$$

Replacing Eq. (13) into Eq. (6), the mass-conservation equation of the species  $\alpha$  in a multicomponent mixture, according to a Fickian law of diffusion, is given by:

$$\frac{\partial(\rho y_\alpha)}{\partial t} + \nabla \cdot (\rho y_\alpha \vec{v}) - \nabla \cdot (\rho \mathcal{D}_{\alpha m} \nabla y_\alpha) = S_{y_\alpha} \quad (14)$$

Similarly, an effective global-diffusion coefficient of species  $\alpha$  in a porous medium,  $\mathcal{D}_\alpha^{\text{eff}}$ , may be derived [34] as:

$$\frac{1}{\mathcal{D}_\alpha^{\text{eff}}} = \frac{1 - \gamma x_\alpha}{\mathcal{D}_{\alpha m}^{\text{eff}}} + \frac{1}{\mathcal{D}_{K\alpha}^{\text{eff}}} \quad (15)$$

In previous SOFCs simulation works [22,23,38,39,41]  $\gamma$  is assumed to be zero, despite this being only strictly true for self-diffusion or equimolar counter transfer [34]; then Eq. (15) becomes:

$$\frac{1}{\mathcal{D}_\alpha^{\text{eff}}} = \frac{1}{\mathcal{D}_{\alpha m}^{\text{eff}}} + \frac{1}{\mathcal{D}_{K\alpha}^{\text{eff}}} \quad (16)$$

Here,  $\mathcal{D}_{\alpha m}^{\text{eff}}$  is the effective binary diffusion coefficient of species  $\alpha$  in the mixture in the porous medium:

$$\mathcal{D}_{\alpha m}^{\text{eff}} = \frac{\varepsilon}{\tau} \mathcal{D}_{\alpha m} \quad (17)$$

where  $\varepsilon$  and  $\tau$  are the porosity and the tortuosity factor of the porous medium, and  $\mathcal{D}_{\alpha m}$  is given by Eq. (12). Likewise, in Eq. (16)  $\mathcal{D}_{K\alpha}^{\text{eff}} = (\varepsilon/\tau) \mathcal{D}_{K\alpha}$ , where  $\mathcal{D}_{K\alpha}$  represents the Knudsen diffusion coefficient of species  $\alpha$  (see Section 2.5). From Eqs. (10) and (16), the Fickian law for the ordinary and Knudsen diffusion flux of the species  $\alpha$  in a multicomponent mixture within a porous media is:

$$\vec{j}_\alpha = -\rho \mathcal{D}_\alpha^{\text{eff}} \nabla y_\alpha \quad (18)$$

Replacing Eq. (18) into Eq. (7), the mass-conservation equation of the species  $\alpha$  in a multicomponent mixture flowing through a porous medium, according to a Fickian diffusion, is given by:

$$\frac{\partial(\varepsilon \rho y_\alpha)}{\partial t} + \nabla \cdot (\rho y_\alpha \langle \vec{v} \rangle) - \nabla \cdot (\rho \mathcal{D}_\alpha^{\text{eff}} \nabla y_\alpha) = S_{y_\alpha} \quad (19)$$

#### 2.4.2. Stefan–Maxwell model

The Stefan–Maxwell (SM) model for diffusion is the most general approach for describing multicomponent mass transport. In contrast to Fick's model, it allows to reproduce typical diffusive effects of ternary mixtures, which are not present in binary diffusion, such as counter diffusion. In the limit of binary mixtures the Stefan–Maxwell model reduces to the Fick's model. In addition, the derivation of the Stefan–Maxwell model is thermodynamically sound, in comparison to the phenomenological formulation of Fick's equation. The Stefan–Maxwell equation can be moreover formulated to take into account the effect of external body forces, as well as to consider the effect of non-equilibrium behaviors of the fluid, such as rarefaction.

Based on the previous work of García-Camprubí et al. [42], a new method to handle the solution of the Stefan–Maxwell equations has been developed. The model is derived by considering the generic driving force of a gas, which is obtained from the differential definition of the internal energy ( $U$ ) in mechanical and thermal equilibrium:

$$dU = T dS - p dV + \sum_{\alpha} \mu_{\alpha} d\mathfrak{N}_{\alpha} \quad (20)$$

where  $T$  is the temperature,  $S$  is the entropy,  $V$  is the volume,  $\mu_{\alpha}$  the chemical potential and  $\mathfrak{N}_{\alpha}$  stands for the number of molecules of species  $\alpha$ . From Eq. (20) we can express the variation of entropy as:

$$dS = \left(\frac{1}{T}\right) dU + \left(\frac{p}{T}\right) dV + \sum_{\alpha} \left(-\frac{\mu_{\alpha}}{T}\right) d\mathfrak{N}_{\alpha} \quad (21)$$

where  $(1/T)$ ,  $(p/T)$  and  $(-\mu_{\alpha}/T)$  are the thermal, mechanical and chemical drivers respectively. Considering an ideal gas, a single component and the Euler's homogeneous function theorem applied to the extensive thermodynamic variables, Eq. (21) yields:

$$d\left(\frac{\mu_{\alpha}}{T}\right) = -\frac{C_{v,\alpha}}{T} dT + \frac{R}{n_{\alpha}} dn_{\alpha} \quad (22)$$

where  $n_{\alpha} = \mathfrak{N}_{\alpha}/V$ ,  $C_{v,\alpha}$  is the heat capacity at constant volume of species  $\alpha$ , and  $R$  is the ideal-gas law constant. The integration of Eq. (22) yields:

$$-\frac{\mu_{\alpha}}{T} = C_{v,\alpha} \ln\left(\frac{T}{T_0}\right) - R \ln\left(\frac{n_{\alpha}}{n_0}\right) \quad (23)$$

being  $n_0$  and  $T_0$  arbitrary constants. The thermodynamic definition of the diffusion driver, for the isothermal case with  $T_0 = T$ , considering  $n_0 = 1$  and linearizing the solution around  $T_0$ , is given by:  $\mu_{\alpha}/T = R p_{\alpha}$ , where  $p_{\alpha}$  is the partial pressure of the species  $\alpha$ . Therefore, we obtain:

$$\nabla\left(\frac{\mu_{\alpha}}{T}\right)_T = R \nabla p_{\alpha} \quad (24)$$

Notice that this is strictly valid for the isothermal case and for those non-isothermal cases where thermodiffusion is negligible. From an asymptotic expansion as a function of the Knudsen number [43], the partial-pressure gradient can be expressed as the sum of the pressure gradients due to diffusive and viscous effects:

$$\nabla p_{\alpha} = \nabla p_{\alpha}^d + \nabla p_{\alpha}^v \quad (25)$$

An expression for the diffusive effects is obtained from the balance between the driving force and the friction between molecules of different species [44]:

$$\nabla p_{\alpha}^d = p \sum_{\beta \neq \alpha} \frac{x_{\alpha} x_{\beta}}{\mathcal{D}_{\alpha\beta}} (\vec{v}_{\beta} - \vec{v}_{\alpha}) \quad (26)$$

which is the Stefan–Maxwell equation for the diffusive flux of a multicomponent mixture, where  $x_{\alpha}$  is the molar fraction of species  $\alpha$ ,  $\vec{v}_{\alpha}$  is the velocity of the species  $\alpha$ , and  $\alpha$  and  $\beta$  stands for all the gaseous components of the mixture. On the other hand, the viscous component of the partial-pressure gradient appears in the momentum equation for the species:

$$\rho_{\alpha} \left( \frac{D\vec{v}_{\alpha}}{Dt} - \nu \nabla^2 \vec{v}_{\alpha} \right) + \nabla p_{\alpha}^v = \rho_{\alpha} \vec{a}_{\alpha} \quad (27)$$

where  $\rho_{\alpha} = \rho y_{\alpha}$ ,  $D/Dt$  is the substantial derivative,  $\nu$  is the kinematic viscosity of the fluid and  $\vec{a}_{\alpha}$  is the acceleration of the species  $\alpha$  due to the presence of external forces. The sum, extended to all the species in the fluid, of Eq. (27) yields:

$$\rho \left( \frac{D\vec{v}}{Dt} - \nu \nabla^2 \vec{v} \right) + \nabla p = \sum_{\alpha} \rho_{\alpha} \vec{a}_{\alpha} \quad (28)$$

In the diffusive limit we have:

$$\frac{D\vec{v}_{\alpha}}{Dt} - \nu \nabla^2 \vec{v}_{\alpha} \approx \frac{D\vec{v}}{Dt} - \nu \nabla^2 \vec{v} = \frac{1}{\rho} \left( \sum_{\alpha} \rho_{\alpha} \vec{a}_{\alpha} - \nabla p \right) \quad (29)$$

From Eqs. (27) and (29), the viscous part of the partial-pressure gradient can be thus expressed as:

$$\nabla p_{\alpha}^v = y_{\alpha} \nabla p + \rho_{\alpha} \left( \vec{a}_{\alpha} - \sum_{\alpha} y_{\alpha} \vec{a}_{\alpha} \right) \quad (30)$$

From Eq. (25), recasting Eq. (26) in terms of the molar fluxes ( $\vec{N}_{\alpha} = c_{\alpha} \vec{v}_{\alpha}$ ) and considering Eq. (30) for an inertial system ( $\vec{a}_{\alpha} = 0$ ), we obtain:

$$\frac{1}{RT} \nabla p_{\alpha} = \sum_{\beta \neq \alpha} \frac{x_{\alpha} \vec{N}_{\beta} - x_{\beta} \vec{N}_{\alpha}}{\mathcal{D}_{\alpha\beta}} + \frac{1}{RT} y_{\alpha} \nabla p \quad (31)$$

which is the Stefan–Maxwell equation consistent with the momentum equation, Eq. (1). Eq. (31) can be usefully re-arranged (as shown in [42]) by leaving the flux of species  $\alpha$ ,  $N_{\alpha}$  on the left-hand side, and introducing by convenience the variables  $\Gamma_{\alpha}^{SM}$ ,  $\vec{v}_{\alpha}^{pSM}$  and  $\vec{v}_{\alpha}^{N^{SM}}$ :



$$\vec{N}_\alpha = -\Gamma_\alpha^{SM} \nabla p_\alpha + \vec{v}_\alpha^{pSM} p_\alpha + \vec{v}_\alpha^{NSM} p_\alpha \quad (32)$$

where  $\Gamma_\alpha^{SM}$ ,  $\vec{v}_\alpha^{pSM}$ ,  $\vec{v}_\alpha^{NSM}$  are given by

$$\Gamma_\alpha^{SM} = \frac{1}{RT \sum_{\beta \neq \alpha} \left( \frac{x_\beta}{D_{\alpha\beta}} \right)} \quad (33)$$

$$\vec{v}_\alpha^{pSM} = \frac{\Gamma_\alpha^{SM} W_\alpha}{W_m p} \nabla p \quad (34)$$

$$\vec{v}_\alpha^{NSM} = \frac{\Gamma_\alpha^{SM} RT}{p} \sum_{\beta \neq \alpha} \frac{\vec{N}_\beta}{D_{\alpha\beta}} \quad (35)$$

Note that the Stefan–Maxwell equation is expressed in terms of molar fluxes and molar fractions, instead of mass flux and mass fractions as required in Eq. (6). For convenience, the chemical species conservation equation is here rearranged in order to cast it in a molar basis. Dividing Eq. (6) by the molecular weight of the species  $\alpha$ , the chemical-species conservation equation becomes:

$$\frac{\partial c_\alpha}{\partial t} + \nabla \cdot (c_\alpha \vec{v}) + \nabla \cdot \vec{J}_\alpha = S_{x_\alpha} \quad (36)$$

which in terms of total molar fluxes is:

$$\frac{\partial c_\alpha}{\partial t} + \nabla \cdot \vec{N}_\alpha = S_{x_\alpha} \quad (37)$$

From Eqs. (37) and (32), the conservation equation of the species  $\alpha$  according to the Stefan–Maxwell model is given by:

$$\frac{\partial c_\alpha}{\partial t} - \nabla \cdot (\Gamma_\alpha^{SM} \nabla p_\alpha) + \nabla \cdot (\vec{v}_\alpha^{pSM} p_\alpha) + \nabla \cdot (\vec{v}_\alpha^{NSM} p_\alpha) = S_{x_\alpha} \quad (38)$$

The set of equations given by Eq. (32) applied to all the species in the fluid but one, together with the momentum and continuity equations given by Eqs. (1) and (4), is the set of equation required to solve the multicomponent mass transfer in a fluid flowing through a channel. Notice that for gases the Stefan–Maxwell diffusion coefficient is equal to the binary diffusion coefficient used for Fick's law, given in Section 2.5. For liquids and dense gases the binary coefficient diffusion should be corrected [44].

#### 2.4.3. Dusty gas model

The dusty-gas model (DGM) describes the global transport of gases through porous media. A full Chapman–Enskog kinetic theory treatment is given for a gas mixture in which the porous medium is considered as one component of the mixture; the pressure variation is then formally equivalent to variation of the solid mole fraction. The DGM states that the gas transport through porous media is due to three independent mechanisms: Knudsen flow, viscous flow and continuum diffusion. The general form of the DGM, neglecting the effects of external forces and thermodiffusion [24], is as follows:

$$-\frac{1}{RT} \nabla p_\alpha = \sum_{\beta \neq \alpha} \frac{x_\beta \vec{N}_\alpha - x_\alpha \vec{N}_\beta}{D_{\alpha\beta}^{eff}} + \frac{\vec{N}_\alpha}{D_{K\alpha}^{eff}} + \frac{1}{D_{K\alpha}^{eff}} \frac{p_\alpha}{RT} \frac{B_0}{\mu} \nabla p \quad (39)$$

Eq. (39) can be recast using the same procedure as for Eq. (31) as:

$$\vec{N}_\alpha = -\Gamma_\alpha^{DGM} \nabla p_\alpha + \vec{v}_\alpha^{pDGM} p_\alpha + \vec{v}_\alpha^{NDGM} p_\alpha \quad (40)$$

where:

$$\Gamma_\alpha^{DGM} = \frac{1}{RT \left[ \sum_{\beta \neq \alpha} \left( \frac{p_\beta}{p D_{\alpha\beta}^{eff}} \right) + \frac{1}{D_{K\alpha}^{eff}} \right]} \quad (41)$$

$$\vec{v}_\alpha^{pDGM} = \frac{\Gamma_\alpha^{DGM}}{D_{K\alpha}^{eff}} \left( -\frac{B_0}{\mu} \nabla p \right) \quad (42)$$

$$\vec{v}_\alpha^{NDGM} = \Gamma_\alpha^{DGM} RT \sum_{\beta \neq \alpha} \left( \frac{\vec{N}_\beta}{p D_{\alpha\beta}^{eff}} \right) \quad (43)$$

The physical meaning and relative importance of  $\Gamma_\alpha^{DGM}$ ,  $\vec{v}_\alpha^{pDGM}$  and  $\vec{v}_\alpha^{NDGM}$  were investigated in [17,45]. Finally, replacing Eq. (40) into Eq. (7) expressed in terms of molar fluxes, we have:

$$\frac{\partial(\varepsilon c_\alpha)}{\partial t} - \nabla \cdot (\Gamma_\alpha^{DGM} \nabla p_\alpha) + \nabla \cdot (\vec{v}_\alpha^{pDGM} p_\alpha) + \nabla \cdot (\vec{v}_\alpha^{NDGM} p_\alpha) = S_{x_\alpha} \quad (44)$$

which is the chemical-species conservation-equation in the porous media according to the dusty gas model. Eq. (44) applied to all the components of the gas mixture represents the complete set of equations for steady-state mass transport, and does not need to be supplemented by any additional equations of motion [24].

The DGM is considered to be the most convenient approach to model the gas transport through porous media [44] and within the SOFC electrodes [20]. Therefore, it is increasingly used for SOFC modeling [13,17]. However, it is worth noting that the theoretical basis

of the DGM [24] was criticized by Kerkhof in [46,47], who as an alternative proposed the binary-friction model (BFM). The experimental data of Evans et al. [48,49] were used to validate the BFM and the DGM; both models showed similar agreement and discrepancies with the measured data [46]. Moreover, Vural et al. [50] have recently reported similar predictions of both models for the concentration overpotential of a SOFC.

## 2.5. Diffusion-coefficient modeling

Experimental data for diffusivities is scarce and the diffusion coefficients must be often calculated using the theoretical or empirical correlations introduced in this subsection. Nevertheless, experimental diffusivity values must be used, when possible, because measurement errors are typically less than those associated with the predictions of empirical or even semi-theoretical equations [51]. In the present work, the measured data for  $\mathcal{D}_{\alpha\beta}$  and  $\mathcal{D}_{K\alpha}$  may be directly taken as a constant.

### 2.5.1. Chapman–Enskog model

The Chapman–Enskog correlation, based on the Kinetic Theory of Gases, is the most common method for theoretically estimating the binary diffusivity [35,52]. It has been widely used for SOFC simulation [21,53,54]. The original expression of the Chapman–Enskog correlation is:

$$\mathcal{D}_{\alpha\beta} = \frac{0.001858T^{1.5}(\frac{1}{W_\alpha} + \frac{1}{W_\beta})^{0.5}}{p\sigma_{\alpha\beta}^2\Omega_D} \quad (45)$$

where  $\mathcal{D}_{\alpha\beta}$  is given in square centimeters per second, the temperature in Kelvin, the molecular weight of species  $\alpha$  in kilogram per kilomole and the total pressure in atmospheres; the average collision diameter in angstroms, calculated as:

$$\sigma_{\alpha\beta} = \frac{\sigma_\alpha + \sigma_\beta}{2} \quad (46)$$

where the value of  $\sigma_\alpha$  is tabulated for the most common species in [55]; and  $\Omega_D$  is the dimensionless collision integral in the Lennard-Jones 12-6 potential model:

$$\Omega_D = \frac{1.06036}{T_N^{0.15610}} + \frac{0.19300}{\exp(0.47635T_N)} + \frac{1.03587}{\exp(1.52996T_N)} + \frac{1.76474}{\exp(3.89411T_N)} \quad (47)$$

Here:

$$T_N = \frac{T}{E_{\alpha\beta}} \quad (48)$$

with  $T$  the temperature and  $E_{\alpha\beta} = \varepsilon_{\alpha\beta}/k_B$ ;  $k_B$  is the Boltzmann constant,  $\varepsilon_{\alpha\beta} = (\sqrt{\varepsilon_\alpha\varepsilon_\beta})$ ; and  $\varepsilon_\alpha$  is the characteristic Lennard-Jones energy. For the most common gases the value of  $E_{\alpha\beta}$  is tabulated in [55]. For convenience we define a new variable  $W_{\alpha\beta}$ , which represents an equivalent molecular weight of the species  $\alpha$  and  $\beta$ :

$$W_{\alpha\beta} = \left(\frac{1}{W_\alpha} + \frac{1}{W_\beta}\right)^{-1} = \frac{W_\alpha W_\beta}{W_\alpha + W_\beta} \quad (49)$$

Replacing Eq. (49) into Eq. (45) we have:

$$\mathcal{D}_{\alpha\beta} = \frac{0.001858T^{1.5}(W_{\alpha\beta})^{-0.5}}{p\sigma_{\alpha\beta}^2\Omega_D} \quad (50)$$

Because of unit consistency, Eq. (50) is modified as follows:

$$\mathcal{D}_{\alpha\beta} = 10.1325 \frac{0.001858T^{1.5}(W_{\alpha\beta})^{-0.5}}{p\sigma_{\alpha\beta}^2\Omega_D} \quad (51)$$

Eq. (51) differs from Eq. (45) in the units of the total pressure and the binary diffusion coefficient; here, SI units apply (Pa, m<sup>2</sup> s<sup>-1</sup>).

### 2.5.2. Wilke–Lee model

The Wilke–Lee correlation for the binary diffusion model is given by [56]:

$$\mathcal{D}_{\alpha\beta} = \frac{(0.0027 - 0.0005(\frac{W_\alpha + W_\beta}{W_\alpha W_\beta})^{0.5})T^{1.5}(\frac{W_\alpha + W_\beta}{W_\alpha W_\beta})^{0.5}}{p\sigma_{\alpha\beta}^2\Omega_D} \quad (52)$$

where  $\mathcal{D}_{\alpha\beta}$  is expressed in square centimeters per second, the molecular weight is expressed in kilogram per kilomole, the temperature is in Kelvin, and the pressure is in atmospheres;  $\sigma_{\alpha\beta}$  is defined in Eq. (46) where the collision diameters must be introduced in angstroms; and the collision integral (dimensionless) is defined by Eq. (47).

Introducing Eq. (49) into Eq. (52) we have:

$$\mathcal{D}_{\alpha\beta} = \frac{(0.0027 - 0.0005W_{\alpha\beta}^{-0.5})T^{1.5}W_{\alpha\beta}^{-0.5}}{p\sigma_{\alpha\beta}^2\Omega_D} \quad (53)$$



To convert the units of the binary ordinary-diffusion coefficient and the pressure into the SI system ( $\text{m}^2 \text{s}^{-1}$ , Pa) Eq. (53) is modified as follows:

$$\mathcal{D}_{\alpha\beta} = 10.1325 \frac{(0.0027 - 0.0005 W_{\alpha\beta}^{-0.5}) T^{1.5} W_{\alpha\beta}^{-0.5}}{p \sigma_{\alpha\beta}^2 \Omega_D} \quad (54)$$

where  $\sigma_{\alpha\beta}$  is the only parameter that is not expressed in SI system units, as it remains in angstroms.

### 2.5.3. Fuller–Schettler–Giddings model

The Fuller–Schettler–Giddings empirical correlation is the simplest correlation to use and it is reported to be more accurate for the prevailing SOFC operating conditions [57]; it is thus widely used for SOFCs simulation [14,16,38]. The Fuller–Schettler–Giddings empirical correlation for the binary diffusivity ( $\mathcal{D}_{\alpha\beta}$ ) of non-polar gases at low pressures is [35,58]:

$$\mathcal{D}_{\alpha\beta} = \frac{0.001 T^{1.75} (\frac{1}{W_\alpha} + \frac{1}{W_\beta})^{0.5}}{p [(\Sigma v)_\alpha^{1/3} + (\Sigma v)_\beta^{1/3}]^2} \quad (55)$$

where  $\Sigma v$  is the diffusion volume,  $\mathcal{D}_{\alpha\beta}$  is given in square centimeters per second, the temperature in Kelvin, the molecular weight of the species- $\alpha$  in kilogram per kilomole and the total pressure in atmospheres; the value of the diffusion volume of species  $\alpha$  ( $\Sigma v_\alpha$ ) is tabulated in [34,35].

Substituting Eq. (49) into Eq. (55) we have:

$$\mathcal{D}_{\alpha\beta} = \frac{0.001 T^{1.75} W_{\alpha\beta}^{-0.5}}{p [(\Sigma v)_\alpha^{1/3} + (\Sigma v)_\beta^{1/3}]^2} \quad (56)$$

To convert Eq. (56) to use consistent units, it is modified as follows:

$$\mathcal{D}_{\alpha\beta} = 10.1325 \frac{0.001 T^{1.75} W_{\alpha\beta}^{-0.5}}{p [(\Sigma v)_\alpha^{1/3} + (\Sigma v)_\beta^{1/3}]^2} \quad (57)$$

where the SI units are now used for all the variables involved. Hence, in Eq. (57) the binary diffusion coefficient is expressed in square meters per second, the temperature in Kelvin; the molecular weight in kilogram per kilomole, and the total pressure in Pascal.

### 2.5.4. Knudsen model

The Kinetic Theory of Gases defines the Knudsen diffusion coefficient as [34,52]:

$$\mathcal{D}_{K\alpha} = \frac{d_p}{3} \sqrt{\frac{8RT}{\pi W_\alpha}} \quad (58)$$

where  $\mathcal{D}_{K\alpha}$  is given in SI units if the temperature is expressed in Kelvin, the molecular weight in kilograms per kilomole, the mean pore diameter ( $d_p$ ) in meters and the ideal gas law constant in Joule per kilomole per Kelvin. Eq. (58) is unanimously used for the calculation of the Knudsen diffusivity in the SOFC related literature.

## 3. Overview of the software structure

In the modeling and simulation of phenomena of scientific and technological relevance, open-source codes offer a collaborative platform for the dissemination of new ideas and methodologies and, simultaneously, foster the optimal evolution of state-of-the-art algorithms due to the peer review and control of the source code itself. These benefits speed up the development of design tools and boost the collaboration between code developers and equipment designers, and their mutual feedback.

The work presented in this paper is based on the OpenFOAM® toolbox, an open-source platform for the solution of partial differential equations usually encountered in the mathematical description of continuum mechanics of solids and fluids. This toolbox is an implementation of fast, robust and accurate numerical solvers designed for managing complex geometries using the finite-volume method. It uses the natural language of continuum mechanics, representing the equations in a straightforward way, as shown in Algorithm 1.

OpenFOAM® has an object-oriented design and is written in C++, which provides one of its most useful features: the extension of the modeling capabilities in the form of libraries, such as the one introduced in this paper and intended to address the simulation of SOFCs. It encompasses two separate items. These are: a *library* (Section 4.1) embodying the mass-transfer models; and a *solver* (Section 4.2), which handles the definition of the SOFC domains, the SOFC models and their coupling.

## 4. Description of the individual software components

### 4.1. Multi-species mass-transfer library

Multi-species mass-transport is not only a key sub-model in a SOFC simulation but it is also required for the numerical solution of a wide range of industrial processes (e.g. catalytic converters, or chemical-vapor deposition). However, OpenFOAM® does not include a general multi-species mass-transport code (as of version 1.6-ext or 1.7.x). To fill this gap, the authors have developed a multi-species mass-transfer library following the OpenFOAM® conventions and philosophy. The library contains the most widely used multi-species mass-transport models in the literature, which were introduced in Section 2. A graphical description of the library contents and structure is shown in Fig. 2; it is divided in four major blocks described below.

```
// Generic equation:
```

$$\frac{\partial \rho \vec{v}}{\partial t} + \nabla \cdot (\rho \vec{v} \vec{v}) - \nabla \cdot \mu (\nabla \vec{v}) = -\nabla p$$

```
// OpenFOAM code:
```

```
solve
(
    fvm::ddt(rho, U)
  + fvm::div(phi, U)
  - fvm::laplacian(mu, U)
  ==
  - fvc::grad(p)
)
```

**Algorithm 1:** Typical implementation of a partial differential equation in OpenFOAM®.

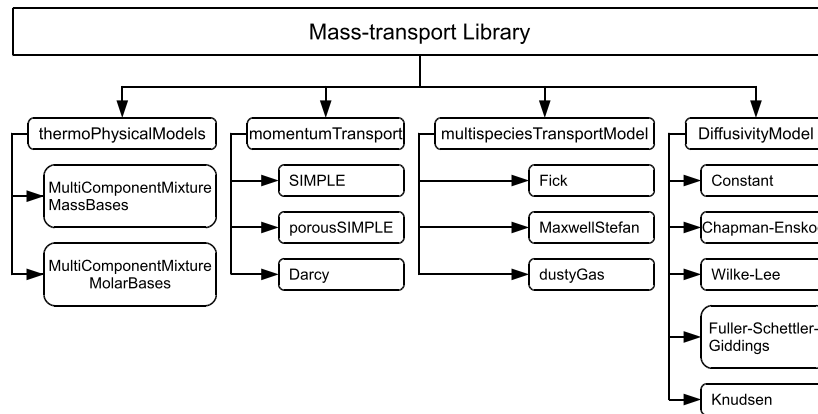


**Fig. 2.** Structure of the mass-transport library for OpenFOAM®.

#### 4.1.1. Thermophysical models

The thermoPhysicalModels is the library database, and consists of the following classes: (i) multiComponentMixtureMassBases; and (ii) multiComponentMixtureMolarBases.

Both classes store all the required variables to characterize a mixture of species  $\alpha$  ( $y_\alpha, x_\alpha, n_\alpha, N_\alpha$  and  $W_m$ ) as well as the functions correct and the functions to update the fluxes (correctMolarFluxes and correctMassFluxes respectively). As it is shown in Section 2.4, the species mass conservation equation changes depending on the chosen diffusion model, as it also does the dependent variable to be solved ( $y_\alpha$  for Fickian models and  $p_\alpha$  for Stefan–Maxwell and dusty-gas models). Therefore, each diffusion model recalls the proper mixture class (models that use  $p_\alpha$  are based on multiComponentMixtureMolarBases). The function correct contains the correlations needed to calculate the mixture molar weight and the remain composition variables (from mass fractions to molar fractions for multiComponentMixtureMassBases and from molar fractions to mass fractions for multiComponentMixtureMolarBases). Both classes work like a base for a standard OpenFOAM® thermodynamic model in which all mixture properties are defined ( $c_p, \alpha$ , etc.).

#### 4.1.2. Momentum-continuity models

This block is based on the class momentumTransport, which includes the structure to account for momentum and mass conservation. The derived classes are: (i) SIMPLE; (ii) porousSIMPLE; and (iii) Darcy.

SIMPLE contains the code to solve Eqs. (1) and (4) using the SIMPLE velocity-pressure algorithm implemented in rhoSimpleFoam, a standard solver of OpenFOAM®.

porousSIMPLE solves Eqs. (2) and (5) as it is done in the standard OpenFOAM® solver rhoPorousSimpleFoam.

Darcy solves Eqs. (3) that is the common form of the Darcy Law.

#### 4.1.3. Mass-transfer models

In Algorithm 2, the structure of the class multiSpeciesTransportModel is shown. This handles the solution of the chemical species conservation equation for a given diffusion model (see Section 2.4) either in a channel or in a porous media. The derived classes from multiSpeciesTransportModel, named after the mass-diffusion model, are: (i) Fick; (ii) MaxwellStefan; and (iii) dustyGas.

The Fick class allows the user to specify which of the three possible Fickian species-conservation equations must be considered: Eq. (11) for binary mixtures; Eq. (14) for multicomponent mixtures; or Eq. (19) for multicomponent mixtures in a porous medium. As shown in Algorithm 2, the procedure of this subroutine is as follows: (a) it solves the momentum and continuity equations, calling the class momentumTransport::SIMPLE or momentumTransport::porousSIMPLE depending on the medium; (b) it solves the selected mass-conservation equation for  $(N - 1)$  species; (c) it calculates the total mass fluxes,  $\vec{n}_\alpha$ ; (d) it calculates the value of the non-solved-for species ensuring continuity; (e) it updates the molar bases fields, calling the update functions of multiComponentMixtureMassBases; and (f) it updates the diffusion coefficients with the class diffusivityModel.

```

multiSpeciesTransportModel::solve()
{
  if (Fick or MaxwellStefan)
    momentumTransport::momentumLoop()
    {
      if (porous)
        momentumTransport::porousSIMPLE
      else (channels)
        momentumTransport::SIMPLE
      endif
    }
  endif
  massTransportLoop()
  {
    if (Fick or MaxwellStefan)
      for (  $\alpha = 1; \alpha < (N-1); \alpha++$  )
        speciesEquation.solve()  $\rightarrow y_\alpha$  or  $p_\alpha$ 
        speciesEquation.flux()  $\rightarrow \bar{n}_\alpha$  or  $\bar{N}_\alpha$ 
      endfor
      if (Fick)
         $y_N = 1 - \sum_{(\alpha \neq N)} y_\alpha$ 
         $\bar{n}_N = \rho \bar{v} - \sum_{(\alpha \neq N)} \bar{n}_\alpha$ 
      else (MaxwellStefan)
         $p_N = p - \sum_{(\alpha \neq N)} p_\alpha$ 
         $\bar{N}_N = \rho \bar{v} W_m^{-1} - \sum_{(\alpha \neq N)} \bar{N}_\alpha$ 
         $x_\alpha = p_\alpha / p$ 
      endif
      correct()
      calcCoefficients()
    else (dustyGas)
      for (  $\alpha = 1; \alpha < N; \alpha++$  )
        speciesEquation.solve()  $\rightarrow p_\alpha$ 
        speciesEquation.flux()  $\rightarrow \bar{N}_\alpha$ 
      endfor
       $p = \sum p_\alpha$ 
       $x_\alpha = p_\alpha / p$ 
      correct()
      calcCoefficients()
      momentumTransport::Darcy
    endif
  }
}

```

**Algorithm 2:** Structure of the multiSpeciesTransportModel, the segregated solver to calculate the species mass-transport.

The MaxwellStefan class allows the solution of the multicomponent mass-transfer in a porosity-free domain. The algorithm, also shown in [Algorithm 2](#), is: (a) the class momentumTransport::SIMPLE is called to solve the momentum and continuity equations; (b) Eq. (38) is solved for  $(N-1)$  species; (c) the total molar fluxes,  $\bar{N}_\alpha$ , are calculated; (d) the value of the non-solved-for species is calculated ensuring continuity; (e) molar fractions are calculated from partial pressures; (f) multiComponentMixtureMolarBases update functions are called to update the mass fields; (g) class diffusivityModel is called to update the diffusion coefficients; and (h) the parameters of the species conservation equation ( $\Gamma_\alpha^{SM}, \bar{v}_\alpha^{p^{SM}}, \bar{v}_\alpha^{N^{SM}}$ ) are recalculated.

The dustyGas class contains the algorithm to solve the mass transport through a porous media according to the dusty-gas model. It differs from the ones used in the Fick and MaxwellStefan classes in that it admits only momentumTransport::Darcy. The procedure, shown in [Algorithm 2](#) is: (a) Eq. (44) is solved for all the species of the gas mixture; (b) the total molar fluxes,  $\bar{N}_\alpha$ , are calculated; (c) the total pressure of the fluid is calculated as:  $p = \sum_\alpha p_\alpha$ ; (d) molar fractions are calculated from partial pressures; (e) multiComponentMixtureMolarBases update functions are called to update the mass fields; (f) the diffusivities are recalculated calling the class diffusivityModel; (g)  $\Gamma_\alpha^{DGM}, \bar{v}_\alpha^{p^{DGM}}, \bar{v}_\alpha^{N^{DGM}}$  are updated; and blue(h) the fluid permeation velocity is calculated from Eq. (44).

For the proper performance of the library, a new boundary condition, called fixedFlux, is required. fixedFlux is derived from the OpenFOAM® basic boundary-condition fixedGradientFvPatchField and its implementation follows the standard OpenFOAM® conventions in order to obtain a generic boundary condition applicable for all mass-transport models. Given a generic mass-flux of a species  $\alpha$  normal to a boundary surface ( $\psi_\alpha$ ), fixedFlux calculates the normal gradient of the species ( $snGrad_{\phi_\alpha}$ ) at that boundary according to the chosen diffusion model:

$$snGrad_{\phi_\alpha} = \frac{(v_\alpha^N + v_\alpha^p) \phi_\alpha - \psi_\alpha}{\Gamma_\alpha}. \quad (59)$$

where  $\phi_\alpha$ ,  $\psi_\alpha$ ,  $v_\alpha^N$ ,  $v_\alpha^p$  and  $\Gamma_\alpha$  for the different diffusion models are given in [Table 2](#).

#### 4.1.4. Diffusion-coefficient models

The diffusivityModel is the generic class to compute the diffusivity coefficients. The theoretical or semi-empirical correlations described in [Section 2.5](#) have been implemented in the derived classes: (i) constant to introduce experimental diffusivity values;

**Table 2**Values of the parameters of the `fixedFlux` boundary condition for the several diffusion models.

Diffusion model	$\phi_\alpha$	$\psi_\alpha$	$v_\alpha^p$	$v_\alpha^N$	$\Gamma_\alpha$
Fick (binary)	$y_\alpha$	$(\vec{j}_\alpha \cdot \vec{n})$	0	0	$(\rho \mathcal{D}_{\alpha\beta})$
Fick (multicomponent)	$y_\alpha$	$(\vec{j}_\alpha \cdot \vec{n})$	0	0	$(\rho \mathcal{D}_{\alpha m})$
Fick (porous)	$y_\alpha$	$(\vec{j}_\alpha \cdot \vec{n})$	0	0	$(\rho \mathcal{D}_\alpha^{\text{eff}})$
MaxwellStefan	$p_\alpha$	$(\vec{N}_\alpha \cdot \vec{n})$	$(\vec{v}_\alpha^{pSM} \cdot \vec{n})$	$(\vec{v}_\alpha^{NSM} \cdot \vec{n})$	$\Gamma_\alpha^{SM}$
dustyGas	$p_\alpha$	$(\vec{N}_\alpha \cdot \vec{n})$	$(\vec{v}_\alpha^{pDGM} \cdot \vec{n})$	$(\vec{v}_\alpha^{NDGM} \cdot \vec{n})$	$\Gamma_\alpha^{DGM}$

(ii) Champan-Enskog to calculate  $\mathcal{D}_{\alpha\beta}$  according to Eq. (51); (iii) Wilke-Lee to calculate  $\mathcal{D}_{\alpha\beta}$  according to Eq. (54); (iv) Fuller-Schettler-Giddings to calculate  $\mathcal{D}_{\alpha\beta}$  according to Eq. (57); and (v) Knudsen to calculate  $\mathcal{D}_{K\alpha}$ , given by Eq. (58). The user may select at run time which model to use.

#### 4.2. Integration in a SOFC solver

This section shows how the library provided can be integrated in a CFD simulation code for the prediction of the performance of SOFCs. The resulting software will be referred to as *the SOFC solver*, and represents an example of the capability of the previously described multi-species mass-transport library and it can be further extended by linking it to other libraries (e.g. an eventual thermal sub-model). It should be therefore noted that the SOFC solver is a sample application of the library, and not currently released. The solver has been also written in C++, taking into account the OpenFOAM® code style and fully ensuring its compatibility.

The solver divides the SOFC in five adjacent subdomains, according to its different components: (i) fuel channel; (ii) anode; (iii) electrolyte; (iv) cathode; and (v) air channel. The solver requires one mesh for each of those subdomains to solve the physical phenomena taking place in each component; and thus it also requires a coupling algorithm to transfer information from each mesh to its neighboring ones.

The SOFC solver structure is based on a virtual class called `component`, from which two classes are derived: (i) `solidComponent` to store the properties of a solid material in a class `material`; and (ii) `fluidComponent` which contains the functions to exchange fluid fields between regions. Since a SOFC component may be a fluid, a solid or a mixture of both (e.g. fluid flowing through a porous medium), the following classes have been further derived to model each of the cell components: (a) `channel` derived from `fluidComponent` to model the gas channels (either air or fuel channel); (b) `electrode` to model the porous media of the cell (anode or cathode), it is thus derived from both `fluidComponent` and `solidComponent`; and (c) a class `electrolyte` derived from `solidComponent` to model the impervious solid in the cell (the electrolyte).

Classes `channel` and `electrode` inherit the mass and momentum conservation algorithms from classes `multiSpeciesTransportModel` and `momentumTransport` (see Section 4.1). Since the electrochemical reaction in a SOFC takes place in a very thin region in the vicinity of the electrode-electrolyte interfaces [59], it is considered to take place on a surface and it is thus modeled as a boundary condition, where the gradient of each component of the mixture is calculated applying the `fixedFlux` boundary condition to the molar fluxes given by Faraday's Law:

$$\vec{N}_{\alpha,r} \cdot \vec{n}_r = \frac{I}{nF} \quad (60)$$

where  $I$  is the current density,  $\vec{n}_r$  is the unit vector normal to the reaction boundary,  $n$  is the number of electrons required to convert a single molecule of species  $\alpha$  and  $F$  is Faraday's constant. Since no volumetric reactions are considered, the following relationships are valid at every cell component:  $S_{x_\alpha} = 0$ ,  $S_{y_\alpha} = (S_{x_\alpha} W_\alpha) = 0$ ,  $S_y = (\sum_\alpha S_{y_\alpha}) = 0$ . However, when using the boundary condition `fixedFlux` special care must be taken at the reaction boundaries (electrode-electrolyte interfaces), where the velocity is fixed to zero (electrolyte is an impervious solid) and then  $\vec{N}_{\alpha,r} = \vec{j}_{\alpha,r}$ . It should be noted that  $\sum_\alpha (W_\alpha \vec{j}_{\alpha,r}) \neq 0$ , i.e.  $\sum_\alpha (\vec{j}_{\alpha,r}) \neq 0$ . The reaction boundaries are mass-diffusion inlet-outlets of the cell. This diffusivity-boundary mass source is therefore taken into account when solving the continuity equation in the `momentumTransport` (`surfMassSource`).

On the other hand, mass transport is not solved in the electrolyte, where the conservation of anions is imposed. Therefore, the class `electrolyte` does not contain any `multiSpeciesTransportModel` or `momentumTransport` as the other components do. However, `electrolyte` stores the electrochemical algorithm to solve the electrochemistry of the cell; it is based on the one described in [60]. The electrolyte is modeled like a thin plate, where the current density path is normal to the electrolyte-electrode interface. Either the cell current density or the cell voltage is required as an input in the `electrolyte` class. If the cell voltage is given, the function `updateCurrentDensity()` solves the Butler-Volmer equation and the Ohm law for each element of the mesh to find the current density value that satisfies the imposed voltage. If, on the contrary, the average current density is fixed, then a similar subroutine `updateVoltage()` calculates the cell voltage.

All the above mentioned classes are combined in a top level solver, named `sofcFoam`, that defines the procedure for the solution of the SOFC solver. Fig. 3 shows the flow chart of the SOFC solver algorithm and coupling; and Table 3 gathers the boundary conditions required by the solver. Essentially, `sofcFoam` reads from a file the regions names and creates the respective objects. All these objects are independent and can be independently controlled both in terms of the selection of sub-models and of solution parameters. The solution algorithm is segregated and the most convenient order to solve regions is starting from the inner of the cell. Thus, the electrolyte is solved first, then the electrodes, and finally the gas channels; the process is repeated until convergence. Every time a region is solved, the corresponding elements in the neighboring mesh are updated using the OpenFOAM® `autoMap` class.

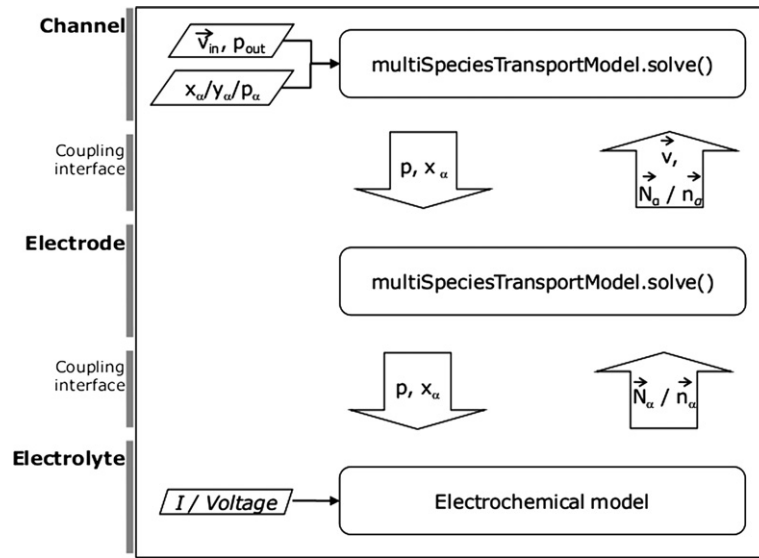


Fig. 3. SOFC solver structure for OpenFOAM®.

**Table 3**  
Boundary conditions required by the SOFC solver.

Channel field	patch	type
Velocity	@inlet	fixedValue (mass flux)
	@outlet	zeroGradient
	@electrode interface	fixedValue (from electrode)
Pressure	@inlet	zeroGradient
	@outlet	fixedValue
	@electrode interface	zeroGradient
Species concentration	@inlet	fixedValue (feeding composition)
	@outlet	zeroGradient
	@electrode interface	fixedFlux (from electrode)
Electrode field	patch	type
Velocity	@channel interface	zeroGradient
	@electrolyte interface	fixedValue (0 0 0)
Pressure	@channel interface	fixedValue (from channel)
	@electrolyte interface	zeroGradient
Species concentration	@channel interface	fixedValue (from channel)
	@electrolyte interface	fixedFlux (Faraday's Law)
Electrolyte field	patch	type
Species concentration	@electrode interface	fixedValue (from electrode)

## 5. Validation and results

### 5.1. Validation of the multi-species mass-transfer library

The performance of the mass-transfer library presented in Section 4.1 is here assessed by comparison with analytical solutions of the mass-transfer models presented in Section 2.4. For this purpose, the well-known Stefan Tube test case (1D, steady-state, multicomponent mass-transfer at constant pressure) is used. Note that in this section the mass or molar fluxes (either  $\vec{n}_\alpha$  or  $N_\alpha$ ) are one-dimensional vectors, in the direction of the tube axis; therefore only the magnitude of the vector is used in the derivation of the analytical solutions ( $n_\alpha$  or  $N_\alpha$ ).

#### 5.1.1. Validation of *Fick*

The analytical solution of Eq. (11) for a non-reacting binary mixture is:

$$y_\alpha(x) = \frac{\frac{n_\alpha W_\alpha}{n_\alpha W_\beta + n_\beta W_\alpha} + \left\{ \frac{y_\alpha(0) W_\alpha}{y_\alpha(0)(W_\beta - W_\alpha) + W_\alpha} - \frac{n_\alpha W_\alpha}{n_\alpha W_\beta + n_\beta W_\alpha} \right\} e^{\left( \frac{(n_\alpha W_\beta + n_\beta W_\alpha) RT x}{W_\beta W_\alpha p D_{\alpha\beta}} \right)}}{1 - \frac{n_\alpha (W_\beta - W_\alpha)}{n_\alpha W_\beta + n_\beta W_\alpha} - \left\{ \frac{y_\alpha(0)(W_\beta - W_\alpha)}{y_\alpha(0)(W_\beta - W_\alpha) + W_\alpha} - \frac{n_\alpha (W_\beta - W_\alpha)}{n_\alpha W_\beta + n_\beta W_\alpha} \right\} e^{\left( \frac{(n_\alpha W_\beta + n_\beta W_\alpha) RT x}{W_\beta W_\alpha p D_{\alpha\beta}} \right)}}} \quad (61)$$

where the following relationships have been used:  $n_\alpha = y_\alpha \rho v - \rho D_{\alpha\beta} \nabla y_\alpha$ ,  $y_\alpha + y_\beta = 1$ ,  $\rho = p W_m / (RT)$  and  $W_m = W_\alpha W_\beta / (y_\alpha (W_\beta - W_\alpha) + W_\alpha)$ . Fig. 4 shows the comparison between the numerical results obtained with the library and the analytical results calculated with Eq. (61), under the conditions given in Table 4.

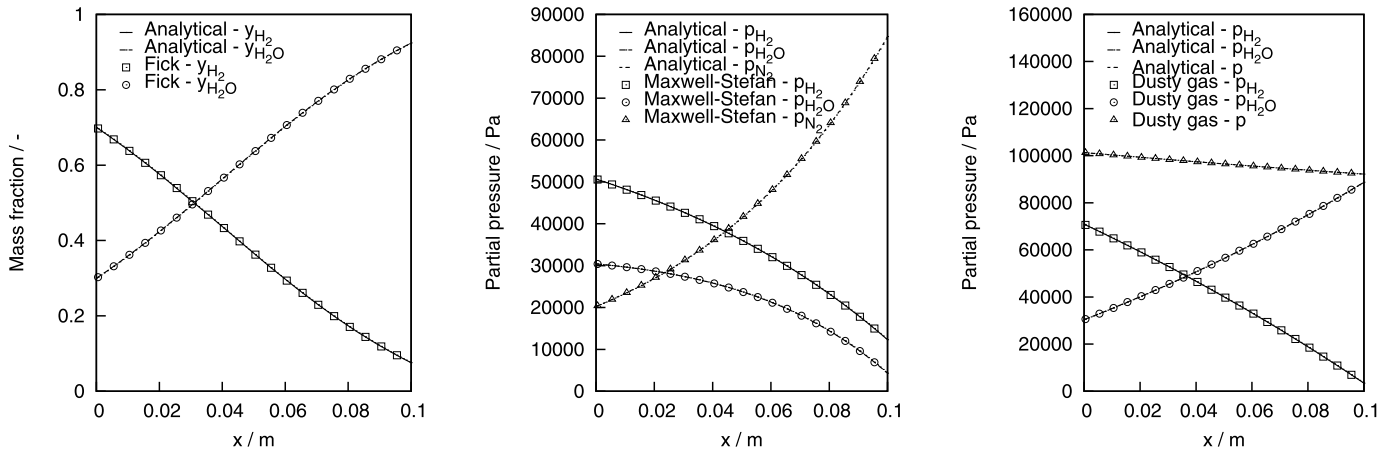


**Fig. 4.** Mass-transfer library: 1D analytical validation of the *FickModel*, the *MaxwellStefanModel* and the *DustyGasModel*.

**Table 4**

Conditions for the validation of the *FickModel* for a binary mixture consisting of  $H_2$  and  $H_2O$ .

Variable	Value
Species ( $\alpha, \beta$ )	$H_2, H_2O$
Tube length	0.1 m
Temperature	1073 K
Pressure	101 325 Pa
$y_{H_2}(0)$	0.7
$y_{H_2O}(0)$	0.3
$n_{H_2}(0.1)$	$5e-4 \text{ kg m}^{-2} \text{ s}^{-1}$
$n_{H_2O}(0.1)$	$0 \text{ kg m}^{-2} \text{ s}^{-1}$
$\mathcal{D}_{\alpha\beta}$	Fuller–Schettler–Giddings

### 5.1.2. Validation of *MaxwellStefan*

From Eq. (31) the Stefan–Maxwell equations for the steady-state multicomponent diffusion under constant pressure are:

$$\nabla p_\alpha = RT \sum_{\beta} \frac{\vec{N}_\beta p_\alpha - \vec{N}_\alpha p_\beta}{p \mathcal{D}_{\alpha,\beta}} \quad (62)$$

For the Stefan Tube test (1D), we can write Eq. (62) in matrix form as follows:

$$\frac{dp_\alpha}{dx} = D_{\alpha,\beta} p_\alpha + M_\alpha \quad (63)$$

Defining  $\Lambda_{\alpha,\beta} = S_{\alpha,\beta} D_{\alpha,\beta} S_{\alpha,\beta}^{-1}$ , where  $\Lambda_{\alpha,\beta}$  is a diagonal matrix containing the eigenvalues ( $\lambda_\alpha$ ) of the matrix  $D_{\alpha,\beta}$ , and  $S_{\alpha,\beta}$  is the corresponding eigenvectors matrix, and using the auxiliary variables  $q_\alpha = S_{\alpha,\beta} p_\alpha$  and  $G_\alpha = S_{\alpha,\beta} M_\alpha$ , the system of equations (63) can be written in the form:

$$\frac{dq_\alpha}{dx} = \lambda_\alpha q_\alpha(x) + G_\alpha \quad (64)$$

the solution of which is:

$$q_\alpha(x) = \left[ q_\alpha(0) + \frac{G_\alpha}{\lambda_\alpha} \right] \exp(\lambda_\alpha x) - \frac{G_\alpha}{\lambda_\alpha} \quad (65)$$

In the case of a ternary mixture (species:  $\alpha, \beta, \gamma$ ) in 1D, the system of Eqs. (62) may be expressed as:

$$\frac{dp_\alpha}{dx} = \frac{RT}{p} \left[ \left( \frac{N_\alpha + N_\gamma}{\mathcal{D}_{\alpha\gamma}} + \frac{N_\beta}{\mathcal{D}_{\alpha\beta}} \right) p_\alpha + \left( \frac{N_\alpha}{\mathcal{D}_{\alpha\gamma}} - \frac{N_\alpha}{\mathcal{D}_{\alpha\beta}} \right) p_\beta - \frac{N_\alpha}{\mathcal{D}_{\alpha\gamma}} p \right] \quad (66)$$

$$\frac{dp_\beta}{dx} = \frac{RT}{p} \left[ \left( \frac{N_\beta}{\mathcal{D}_{\beta\gamma}} - \frac{N_\beta}{\mathcal{D}_{\alpha\beta}} \right) p_\alpha + \left( \frac{N_\beta + N_\gamma}{\mathcal{D}_{\beta\gamma}} + \frac{N_\alpha}{\mathcal{D}_{\alpha\beta}} \right) p_\beta - \frac{N_\beta}{\mathcal{D}_{\beta\gamma}} p \right] \quad (67)$$

$$p_\gamma = p - p_\alpha - p_\beta \quad (68)$$

the analytical solution of which is given by Eq. (65) and the following parameters:



**Table 5**

Conditions for the validation of the `MaxwellStefanModel` for a multicomponent mixture consisting of  $\text{H}_2$ ,  $\text{H}_2\text{O}$  and  $\text{N}_2$ .

Variable	Value
Species ( $\alpha, \beta, \gamma$ )	$\text{H}_2, \text{H}_2\text{O}, \text{N}_2$
Tube length	0.1 m
Temperature	1073 K
Pressure	101 325 Pa
$x_{\text{H}_2}(0)$	0.5
$x_{\text{H}_2\text{O}}(0)$	0.3
$x_{\text{N}_2}(0)$	0.2
$N_{\text{H}_2}(0.1)$	$6\text{e-}5 \text{ kmol m}^{-2} \text{ s}^{-1}$
$N_{\text{H}_2\text{O}}(0.1)$	$2\text{e-}5 \text{ kmol m}^{-2} \text{ s}^{-1}$
$N_{\text{N}_2}(0.1)$	$0 \text{ kmol m}^{-2} \text{ s}^{-1}$
$\mathcal{D}_{\alpha\beta}$	Fuller–Schettler–Giddings

**Table 6**

Conditions for the validation of the `DustyGasModel` for a binary mixture consisting of  $\text{H}_2$ ,  $\text{H}_2\text{O}$ .

Variable	Value
Species ( $\alpha, \beta$ )	$\text{H}_2, \text{H}_2\text{O}$
Tube length	0.1 m
Temperature	1073 K
Pressure	101 325 Pa
$x_{\text{H}_2}(0)$	0.7
$x_{\text{H}_2\text{O}}(0)$	0.3
$N_{\text{H}_2}(0.1)$	$5\text{e-}6 \text{ kmol m}^{-2} \text{ s}^{-1}$
$N_{\text{H}_2\text{O}}(0.1)$	$-1\text{e-}6 \text{ kmol m}^{-2} \text{ s}^{-1}$
Porosity	0.32
Tortuosity	3
Pore diameter	1e-6 m
$\mathcal{D}_{\alpha\beta}$	Fuller–Schettler–Giddings
$\mathcal{D}_{K\alpha}$	Knudsen

$$D_{\alpha,\alpha} = \frac{RT}{p} \left( \frac{N_\alpha + N_\gamma}{\mathcal{D}_{\alpha\gamma}} + \frac{N_\beta}{\mathcal{D}_{\alpha\beta}} \right) \quad (69)$$

$$D_{\alpha,\beta} = \frac{RT}{p} \left( \frac{N_\alpha}{\mathcal{D}_{\alpha\gamma}} - \frac{N_\alpha}{\mathcal{D}_{\alpha\beta}} \right) \quad (70)$$

$$D_{\beta,\alpha} = \frac{RT}{p} \left( \frac{N_\beta}{\mathcal{D}_{\beta\gamma}} - \frac{N_\beta}{\mathcal{D}_{\alpha\beta}} \right) \quad (71)$$

$$D_{\beta,\beta} = \frac{RT}{p} \left( \frac{N_\beta + N_\gamma}{\mathcal{D}_{\beta\gamma}} + \frac{N_\alpha}{\mathcal{D}_{\alpha\beta}} \right) \quad (72)$$

$$M_\alpha = -RT \left( \frac{N_\alpha}{\mathcal{D}_{\alpha\gamma}} \right) \quad (73)$$

$$M_\beta = -RT \left( \frac{N_\beta}{\mathcal{D}_{\beta\gamma}} \right) \quad (74)$$

$$\lambda_\alpha = \frac{(D_{\alpha,\alpha} + D_{\beta,\beta}) + \sqrt{(D_{\alpha,\alpha} - D_{\beta,\beta})^2 + 4 D_{\alpha,\beta} D_{\beta,\alpha}}}{\beta} \quad (75)$$

$$\lambda_\beta = \frac{(D_{\alpha,\alpha} + D_{\beta,\beta}) - \sqrt{(D_{\alpha,\alpha} - D_{\beta,\beta})^2 + 4 D_{\alpha,\beta} D_{\beta,\alpha}}}{\beta} \quad (76)$$

For the conditions given in Table 5, the analytical solution of the Stefan Tube test and the numerical results given by the library using the class `MaxwellStefan` are plotted in Fig. 4.

### 5.1.3. Validation of `dustyGas`

The dusty-gas model describes the global mass transfer of a multicomponent gas mixture flowing through a porous media under non-constant pressure. A binary mixture is considered for this test case (species:  $\alpha, \beta$ ). From Eq. (39) the following system of equations is obtained:

$$\frac{dp}{dx} = - \frac{RT \left( \frac{N_\alpha}{\mathcal{D}_{K\alpha}} + \frac{N_\beta}{\mathcal{D}_{K\beta}} \right)}{1 + \frac{B_0}{\mu} \left[ p_\alpha \left( \frac{1}{\mathcal{D}_{K\alpha}} - \frac{1}{\mathcal{D}_{K\beta}} \right) + \frac{p}{\mathcal{D}_{K\beta}} \right]} \quad (77)$$

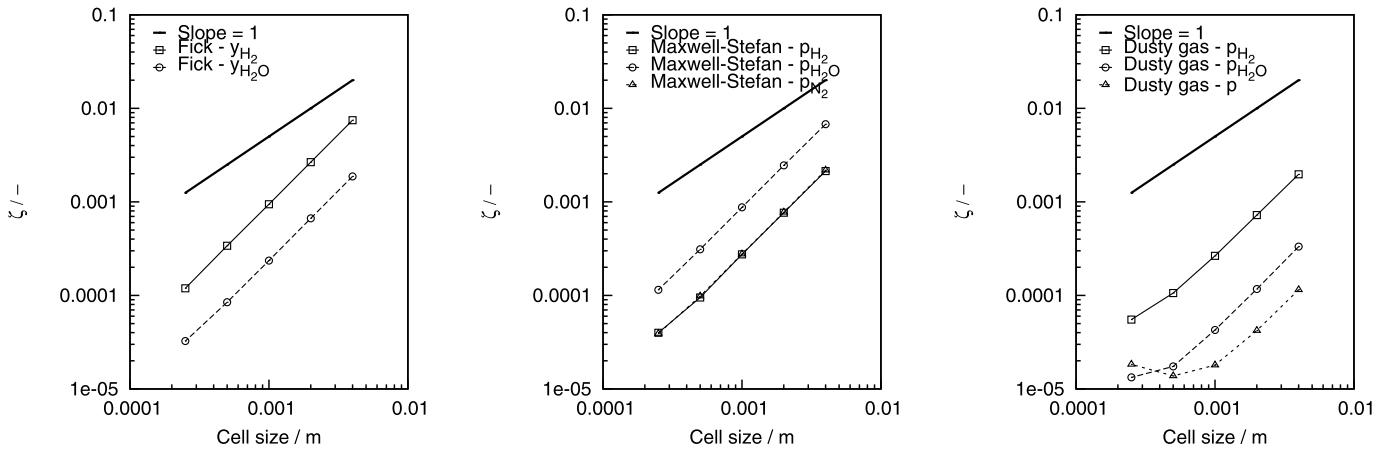


**Fig. 5.** Error as a function of the mesh resolution for FickModel, MaxwellStefanModel and DustyGasModel.

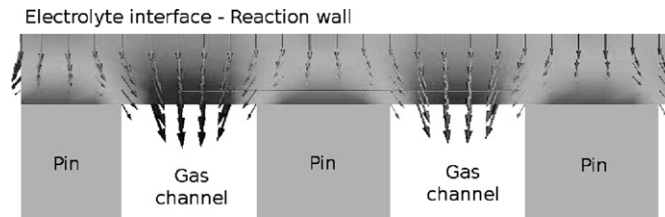


**Fig. 6.** Details of the 2D SOFC geometry.

**Table 7**

Cell parameters: geometry and operating conditions.

Cell geometry	
Cell diameter	78 mm
Anode	Ni/YSZ
Anode thickness	520 μm
Anode porosity	0.32
Anode tortuosity	3
Anode permeability	1e-14 520 m <sup>2</sup>
Cathode	LSCF
Cathode thickness	34 μm
Cathode porosity	0.32
Cathode tortuosity	3
Cathode permeability	1e-14 m <sup>2</sup>
Electrolyte	YSZ
Electrolyte thickness	6 μm
Active area	47 cm <sup>2</sup>
Operating conditions	
Pressure	101 325 Pa
Temperature	700, 750, 800 °C
Fuel flow	0.533 Nl min <sup>-1</sup>
Fuel composition	77% H <sub>2</sub> + 4% H <sub>2</sub> O + 19% N <sub>2</sub>
Air flow	1.5 Nl min <sup>-1</sup>
Air composition	21% O <sub>2</sub> + 79% N <sub>2</sub>

$$\frac{dp_{\alpha}}{dx} = \frac{RT}{pD_{12}}[p_{\alpha}(N_{\alpha} + N_{\beta}) - pN_{\alpha}] - \frac{RT}{pD_{K\alpha}}N_{\alpha} - p_{\alpha} \frac{B_0}{\mu D_{K\alpha}} \nabla p \quad (78)$$

$$\frac{dp_{\beta}}{dx} = \frac{dp}{dx} - \frac{dp_{\alpha}}{dx} \quad (79)$$

This system is solved numerically by scripting the solution procedure in Octave [61,62]. Fig. 4 also shows the comparison between the analytical curves and the numerical results for the dustyGas for the conditions given in Table 6.

Fig. 5 shows the relative errors ( $\zeta$ ) between the reference solutions (analytical or numerical) and the results calculated in this work for all the test cases presented in this section and their dependency with the mesh size. The error is calculated as:

$$\zeta = \frac{\phi_{ref} - \phi_{OpenFOAM}}{\phi_{ref}} \quad (80)$$

The results shown in Fig. 5 further validate the performance of the library.

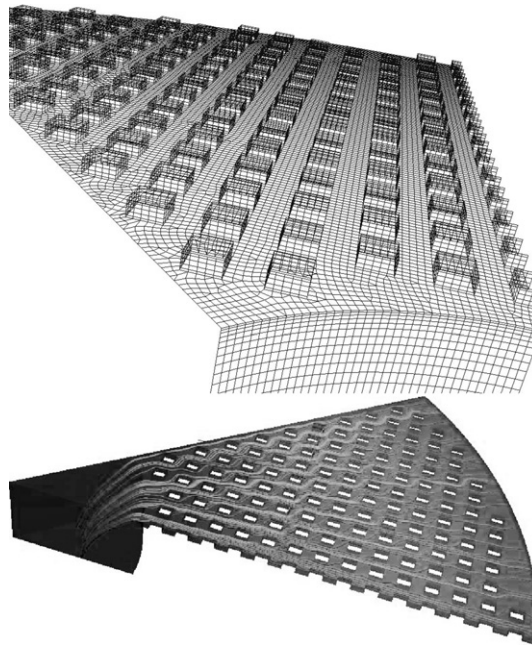


Fig. 7. Details of the 3D SOFC geometry.

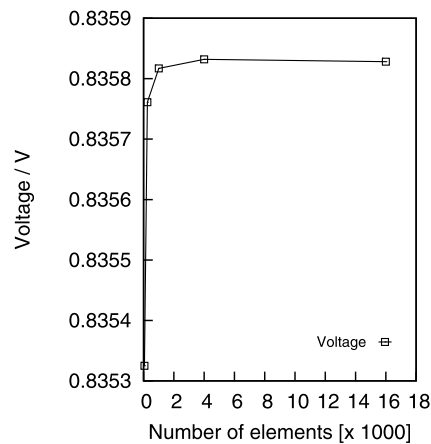


Fig. 8. Mesh dependence of the numerical results for the cell given in Table 7 running at a given mean current density of  $5000 \text{ A m}^{-2}$ .

## 5.2. Validation for a SOFC application

The performance of the `sofcFoam` application introduced in Section 4.2 is shown now by comparison with the experimental data of a circular-shape, planar SOFC; the experimental data have been collected in the authors' (VN, PA) laboratory. The geometry and properties of the cell, as well as the operating conditions, are reported in Table 7. Two approaches for the representation of the cell will be considered: (i) 2D simulations assuming axial symmetry; and (ii) full 3D simulations. Figs. 6 and 7 show some details of the meshes used for both approaches. The meshes were successively refined until the numerical results indicated no dependence on the mesh, as shown in Fig. 8.

Fig. 9 shows the experimental and numerical I–V curves for the cell given in Table 7 at three different operating temperatures. The model fitting parameter is the pre-exponential factor of the cathode current exchange density, which is not kept constant from curve to curve because it is temperature dependent. Good agreement is reached between numerical and experimental data, for both the 2D and 3D simulations.

## 6. Practical issues

### 6.1. Installation instructions

The package `multiSpeciesTransportModels` consists in three folders, namely `lib`, `applications` and `run` and requires a fully functionally installation of OpenFOAM® (version 1.6-ext). In order to install the main software easily, under Ubuntu Lucid 10.04 LTS it is sufficient to add the PPA repository typing in a terminal (superuser privileges are required):

```
sudo add-apt-repository ppa:cae-team/ppa
```

and then

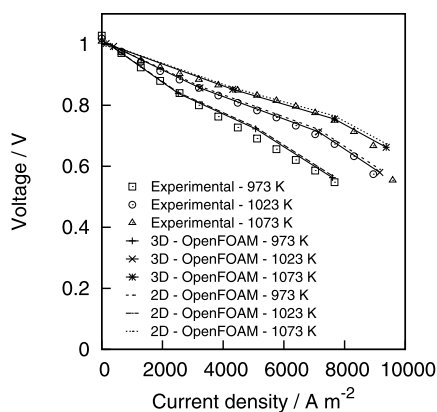


**Fig. 9.** Polarization curves at several temperatures: comparison between experimental data and OpenFOAM® results using the 2D and 3D approaches.

```
sudo apt-get update

sudo apt-get install openfoam-1.6-ext

sudo apt-get install openfoam-1.6-ext-dev

sudo apt-get install binutils-dev

sudo apt-get install g++

sudo apt-get install cmake
```

to install the package satisfying all the dependencies. Finally by typing

```
echo ". /usr/lib/OpenFOAM-1.6-ext/etc/bashrc"
>> ~/.bashrc

echo "export FOAM_USER_APPBIN=
$WM_PROJECT_USER_DIR/applications/bin/$WM_OPTIONS"
>> ~/.bashrc

echo "export FOAM_USER_LIBBIN=
$WM_PROJECT_USER_DIR/lib/$WM_OPTIONS"
>> ~/.bashrc

echo "export PATH=$PATH:$FOAM_USER_APPBIN"
>> ~/.bashrc

echo "export LD_LIBRARY_PATH=
$LD_LIBRARY_PATH:$FOAM_USER_LIBBIN"
>> ~/.bashrc

source ~/.bashrc
```

the installation process will be completed. To install OpenFOAM® under other operating system or to compile it from the source code one can refer the instructions reported on the main web site (<http://www.extend-project.de>). Now for install the multiSpeciesTransportModels create the OpenFOAM® user home folder (if not present) and subfolders with the commands

```
mkdir ~/OpenFOAM

mkdir ~/OpenFOAM/$USER-1.6-ext

mkdir ~/OpenFOAM/$USER-1.6-ext/lib

mkdir ~/OpenFOAM/$USER-1.6-ext/applications

mkdir ~/OpenFOAM/$USER-1.6-ext/run
```

and extract the package in temporary directory (i.e. ~/temp-install) with

```

FoamFile
{
    version      2.0;
    format       ascii;
    class        volScalarField;
    location     "0";
    object       yH2O;
}
// * * * * *

dimensions      [0 0 0 0 0 0 0];

internalField   uniform 0.7;

boundaryField
{
    liquid
    {
        type      fixedValue;
        value      uniform 0.7;
    }
    exit
    {
        type      fixedFlux;
        gradient   uniform 0;
        value      uniform 0.7;
    }
    TreD
    {
        type      empty;
    }
    wall
    {
        type      zeroGradient;
    }
}

```

**Fig. 10.** Initial conditions file for hydrogen mass fraction for Fick validation test case.

```
tar -zxvf multiSpeciesTransportModels.tar.gz
```

Finally by typing

```

cp -r ~/temp-install/mstm/lib/*
~/OpenFOAM/$USER-1.6-ext/lib

cp -r ~/temp-install/mstm/applications/*
~/OpenFOAM/$USER-1.6-ext/applications

cp -r ~/temp-install/mstm/run/*
~/OpenFOAM/$USER-1.6-ext/run

```

copy all the files in the right position. To complete the installation the code has to be compiled. This can be done with the commands

```

~/OpenFOAM/$USER-1.6-ext/lib/allwmake-mstm

~/OpenFOAM/$USER-1.6-ext/applications/allwmake-mstm

```

## 6.2. Test run description

The package multiSpeciesTransportModels contains also a test case reproducing the first validation case reported in Section 5.1 and Fig. 4. Initial conditions are reported in Table 4. All data and parameters are already correctly set. Fig. 10 shows the initial condition file for the hydrogen mass fraction. To see it open the file with any text editor. Using nano text editor type in a terminal

```
nano ~/OpenFOAM/$USER-1.6-ext/run/stefanTube/Fick/0/y_H2
```

(press ctrl+x to exit from the program). Fig. 11 shows the main setting of the multiSpeciesTransportModels library: the diffusion model (Fick), the model for calculating the binary diffusion coefficients (Fuller), the algorithm for the momentum equation (SIMPLE) and the name of the species indirectly calculated (H2O). To run the simulation enter in the case folder with the command

```
cd ~/OpenFOAM/$USER-1.6-ext/run/stefanTube/Fick
```

then generate the mesh with the command

```
blockMesh
```

and finally start the simulation with the command

```

FoamFile
{
    version      2.0;
    format       ascii;
    class        dictionary;
    object       transportProperties;
}
// * * * * *

    multispeciesTransportModel Fick;

    binaryDiffusivityModel     Fuller;

    momentumTransport          SIMPLE;

    inertSpecies                H2O;

// *****

```

**Fig. 11.** TransportProperties dictionary file for Fick validation test case.

```

FoamFile
{
    version      2.0;
    format       ascii;
    class        volScalarField;
    location     "1";
    object       y_H2;
}
// * * * * *

dimensions      [0 0 0 0 0 0];

internalField    nonuniform List<scalar>
100
(
    0.697212
    0.691569
    0.685862
    0.680091
    0.674256
    0.668358
    0.662398
    0.656378
    0.650298
    0.64416
    0.637964
    0.631711
    0.625404
    0.619043
    0.61263
    0.606165
    0.599652
    0.59309
    0.586482
    0.57983
    0.573134
    ...

```

**Fig. 12.** Results file (partial) for hydrogen mass fraction for Fick validation test case.

stefanTube

Fig. 12 shows the content of the results file for the hydrogen mass fraction. To compare it with the own one type in a terminal

```
nano ~/OpenFOAM/$USER-1.6-ext/run/stefanTube/Fick/1/y_H2
```

or check it with any text editor.

## 7. Conclusions

A new mass-transport library has been developed to solve problems involving the multicomponent mass transport through porous media and non-porous domains. A new solver to simulate SOFC performance has also been presented to illustrate the practical use of the mass-transport library.

The library includes the following mass-transport models: (i) *Fick*, for mass-transfer of binary mixtures in non-porous domains; (ii) *Fick*, for mass-transfer of multicomponent mixtures either in non-porous domains or in porous media; (iii) *MaxwellStefan*, for multicomponent mass-transfer in open domains; and (iv) *dustGas*, for multicomponent mass-transfer in porous media. The library also includes the velocity-pressure coupling-algorithms: (a) *SIMPLE* to account for the momentum and mass conservation in non-porous domains; and *porousSIMPLE* to solve the continuity and momentum equations in porous media.



Details of the code structure, both for the library and for the SOFC application, have been provided, paving the way for finding new potential uses and extensions of the library. The modules written in C++ following the standards of OpenFOAM®, to ensure their compatibility.

The accuracy for the developed models has been checked by comparison of the numerical results with analytical solutions (when possible) and with experimental data for actual SOFCs. The satisfactory performance of the library and the SOFC solver has been shown.

## Acknowledgements

The authors acknowledge the work of Marco Pieroni concerning the electrochemistry modules of the library modeling the electrolyte. V.N. acknowledges support by the MULTISS project funded by “Regione Piemonte”. M.G.-C. acknowledges support by the CAI-Europa programme for mobility. S.I. acknowledges support by the Spanish Government through its postdoctoral mobility fellowship programme. This work was partially funded by the Spanish Government under project ENE2008-06683-C03-03.

## References

- [1] International Energy Outlook, Tech. rep., U.S. Energy Information Administration, 2009.
- [2] A.B. Stambouli, E. Traversa, Solid oxide fuel cells (SOFCs): a review of an environmentally clean and efficient source of energy, *Renewable and Sustainable Energy Reviews* 6 (5) (2002) 433–455.
- [3] S.M. Haile, Fuel cell materials and components, *Acta Materialia* 51 (19) (2003) 5981–6000.
- [4] S.C. Singhal, Solid oxide fuel cells for stationary, mobile, and military applications, *Solid State Ionics* 152–153 (2002) 405–410.
- [5] N.Q. Minh, Solid oxide fuel cell technology – features and applications, *Solid State Ionics* 174 (1–4) (2004) 271–277.
- [6] V. Lawlor, S. Griesser, G. Buchinger, A. Olabi, S. Cordiner, D. Meissner, Review of the micro-tubular solid oxide fuel cell: Part i. Stack design issues and research activities, *Journal of Power Sources* 193 (2) (2009) 387–399.
- [7] M.C. Williams, J. Strakey, W. Sudoval, U.S. DOE fossil energy fuel cells program, *Journal of Power Sources* 159 (2) (2006) 1241–1247.
- [8] M. Cali, M. Santarelli, P. Leone, Computer experimental analysis of the CHP performance of a 100 kwe SOFC field unit by a factorial design, *Journal of Power Sources* 156 (2) (2006) 400–413.
- [9] SOFCo acquisition helps Rolls-Royce develop SOFC systems, *Fuel Cells Bulletin* 2007 (6) (2007) 5–6.
- [10] CFCL opens German SOFC manufacturing plant, *Fuel Cells Bulletin* 2009 (10) (2009) 1.
- [11] T. Suzuki, Z. Hasan, Y. Funahashi, T. Yamaguchi, Y. Fujishiro, M. Awano, Impact of anode microstructure on solid oxide fuel cells, *Science* 325 (5942) (2009) 852–855.
- [12] M. Andersson, J. Yuan, B. Sundén, Review on modeling development for multiscale chemical reactions coupled transport phenomena in solid oxide fuel cells, *Applied Energy* 87 (5) (2010) 1461–1476.
- [13] K. Tseronis, I. Kookos, C. Theodoropoulos, Modelling mass transport in solid oxide fuel cell anodes: a case for a multidimensional dusty gas-based model, *Chemical Engineering Science* 63 (23) (2008) 5626–5638.
- [14] D.H. Jeon, J.H. Nam, C.-J. Kim, Microstructural optimization of anode-supported solid oxide fuel cells by a comprehensive microscale model, *Journal of The Electrochemical Society* 153 (2) (2006) A406–A417.
- [15] N. Akhtar, S. Decent, K. Kendall, Numerical modelling of methane-powered micro-tubular, single-chamber solid oxide fuel cell, *Journal of Power Sources* 195 (23) (2010) 7796–7807.
- [16] M.F. Serincan, U. Pasaogullari, N.M. Sammes, Effects of operating conditions on the performance of a micro-tubular solid oxide fuel cell (sofc), *Journal of Power Sources* 192 (2) (2009) 414–422.
- [17] M. García-Camprubí, A. Sánchez-Insa, N. Fueyo, Multimodal mass transfer in solid-oxide fuel-cells, *Chemical Engineering Science* 65 (5) (2010) 1668–1677.
- [18] R. Suwanwarangkul, E. Croiset, M. Pritzker, M. Fowler, P. Douglas, E. Entchev, Mechanistic modelling of a cathode-supported tubular solid oxide fuel cell, *Journal of Power Sources* 154 (1) (2006) 74–85.
- [19] M. Hussain, X. Li, I. Dincer, Mathematical modeling of transport phenomena in porous sofc anodes, *International Journal of Thermal Sciences* 46 (1) (2007) 48–56.
- [20] R. Suwanwarangkul, E. Croiset, M.W. Fowler, P.L. Douglas, E. Entchev, M.A. Douglas, Performance comparison of Fick's, Dusty-Gas and Stefan-Maxwell models to predict the concentration overpotential of a SOFC anode, *Journal of Power Sources* 122 (1) (2003) 9–18.
- [21] S.H. Chan, K.A. Khor, Z.T. Xia, A complete polarization model of a solid oxide fuel cell and its sensitivity to the change of cell component thickness, *Journal of Power Sources* 93 (1–2) (2001) 130–140.
- [22] G.M. Goldin, H. Zhu, R.J. Kee, D. Bierschenk, S.A. Barnett, Multidimensional flow, thermal, and chemical behavior in solid-oxide fuel cell button cells, *Journal of Power Sources* 187 (1) (2009) 123–135.
- [23] T.X. Ho, P. Kosinski, A.C. Hoffmann, A. Vik, Modeling of transport, chemical and electrochemical phenomena in a cathode-supported sofc, *Chemical Engineering Science* 64 (12) (2009) 3000–3009.
- [24] E. Mason, A. Malinauskas, *Gas Transport in Porous Media: The Dusty-Gas Model*, Elsevier, New York, 1983.
- [25] Q. Wang, L. Li, C. Wang, Numerical study of thermoelectric characteristics of a planar solid oxide fuel cell with direct internal reforming of methane, *Journal of Power Sources* 186 (2) (2009) 399–407.
- [26] V.A. Danilov, M.O. Tade, A CFD-based model of a planar SOFC for anode flow field design, *International Journal of Hydrogen Energy* 34 (21) (2009) 8998–9006.
- [27] H. Yakabe, T. Ogiwara, M. Hishinuma, I. Yasuda, 3-D model calculation for planar SOFC, *Journal of Power Sources* 102 (1–2) (2001) 144–154.
- [28] H.-C. Liu, C.-H. Lee, Y.-H. Shiu, R.-Y. Lee, W.-M. Yan, Performance simulation for an anode-supported SOFC using Star-CD code, *Journal of Power Sources* 167 (2) (2007) 406–412.
- [29] D.H. Jeon, A comprehensive CFD model of anode-supported solid oxide fuel cells, *Electrochimica Acta* 54 (10) (2009) 2727–2736.
- [30] OpenCFD, 2010, <http://www.openfoam.com>.
- [31] FoamCFD, 2010, <http://foamcfd.org>.
- [32] S. Izquierdo, J. Valdés, M. Martínez, M. Accolti, S. Woudberg, P. Asinari, M. Miana, J. Du Plessis, Porous-layer model for laminar liquid flow in rough microchannels, *Microfluidics and Nanofluidics* 9 (2010) 1063–1075.
- [33] A.E. Fick, Ueber diffusion, *Poggendorff's Annalen der Physik* 94 (1855) 59.
- [34] J.R. Welty, C.E. Wicks, R.E. Wilson, G. Rohrer, *Fundamentals of Momentum Heat and Mass Transfer*, 4th edition, John Wiley & Sons Inc., 2001.
- [35] E. Cussler, *Diffusion: Mass Transfer in Fluid Systems*, 2nd edition, Cambridge Series in Chemical Engineering, Cambridge University Press, 1997.
- [36] S. Groot, *Thermodynamics of Irreversible Processes*, North-Holland Publishing Co., Amsterdam, 1951.
- [37] R. Bird, W. Stewart, E. Lightfoot, *Transport Phenomena*, revised 2nd edition, John Wiley & Sons, Inc., Amsterdam, 2006.
- [38] D. Bhattacharyya, R. Rengaswamy, C. Finnerty, Dynamic modeling and validation studies of a tubular solid oxide fuel cell, *Chemical Engineering Science* 64 (9) (2009) 2158–2172.
- [39] A.L. Hines, R.N. Maddox, *Mass Transfer: Fundamentals and Applications*, Series in the Physical and Chemical Engineering Sciences, Prentice-Hall, Inc., Englewood Cliffs, NJ, 1985.
- [40] D. Fairbanks, C. Wilke, Diffusion Coefficients in Multicomponent Gas Mixtures, *Industrial and Engineering Chemistry* 42 (3) (1950) 471–475.
- [41] D. Edwards, V. Denny, A. Mills, *Transfer Processes: An Introduction to Diffusion, Convection, and Radiation*, 2nd edition, Series in Thermal and Fluids Engineering, Hemisphere Publishing Corporation, McGraw-Hill, 1979.
- [42] M. García-Camprubí, H. Jasak, N. Fueyo, CFD analysis of cooling effects in H<sub>2</sub>-fed solid oxide fuel cells, *Journal of Power Sources* 196 (17) (2011) 7290–7301.
- [43] P. Asinari, Lattice Boltzmann scheme for mixture modeling: analysis of the continuum diffusion regimes recovering Maxwell-Stefan model and incompressible Navier-Stokes equations, *Phys. Rev. E* 80 (2009) 056701.

- [44] R. Krishna, J.A. Wesselingh, The Maxwell–Stefan approach to mass transfer, *Chemical Engineering Science* 52 (6) (1997) 861–911.
- [45] M. García-Camprubí, N. Fueyo, Mass transfer in hydrogen-fed anode-supported SOFCs, *International Journal of Hydrogen Energy* 35 (20) (2010) 11551–11560.
- [46] P.J.A.M. Kerkhof, A modified Maxwell–Stefan model for transport through inert membranes: The binary friction model, *The Chemical Engineering Journal and the Biochemical Engineering Journal* 64 (3) (1996) 319–343.
- [47] P.J. Kerkhof, M.A. Geboers, Analysis and extension of the theory of multicomponent fluid diffusion, *Chemical Engineering Science* 60 (12) (2005) 3129–3167.
- [48] R.B. Evans, G.M. Watson, J. Truitt, Interdiffusion of gases in a low permeability graphite at uniform pressure, *Journal of Applied Physics* 33 (9) (1962) 2682–2688.
- [49] R.B. Evans, G.M. Watson, J. Truitt, Interdiffusion of gases in a low permeability graphite. II. Influence of pressure gradients, *Journal of Applied Physics* 34 (7) (1963) 2020–2026.
- [50] Y. Vural, L. Ma, D.B. Ingham, M. Pourkashanian, Comparison of the multicomponent mass transfer models for the prediction of the concentration overpotential for solid oxide fuel cell anodes, *Journal of Power Sources* 195 (15) (2010) 4893–4904.
- [51] R.H. Perry, D.W. Green, J.O. Maloney (Eds.), *Perry's Chemical Engineers' Handbook*, 7th edition, McGraw-Hill, 1997.
- [52] S. Chapman, T. Cowling, *The Mathematical Theory of Non-Uniform Gases*, 3rd edition, Cambridge University Press, 1970.
- [53] D. Bhattacharyya, R. Rengaswamy, C. Finnerty, Isothermal models for anode-supported tubular solid oxide fuel cells, *Chemical Engineering Science* 62 (16) (2007) 4250–4267.
- [54] H. Yakabe, M. Hishinuma, M. Uratani, Y. Matsuzaki, I. Yasuda, Evaluation and modeling of performance of anode-supported solid oxide fuel cell, *Journal of Power Sources* 86 (1–2) (2000) 423–431.
- [55] J.O. Hirschfelder, C.F. Curtiss, R.B. Bird, *Molecular Theory of Gases and Liquids*, 4th printing edition, John Wiley & Sons, Inc., New York, 1967.
- [56] C. Wilke, C. Lee, Estimation of diffusion coefficient for gases and vapors, *Industrial & Engineering Chemistry* 47 (1955) 1253–1257.
- [57] B. Todd, J.B. Young, Thermodynamic and transport properties of gases for use in solid oxide fuel cell modelling, *Journal of Power Sources* 110 (1) (2002) 186–200.
- [58] E.N. Fuller, P.D. Schettler, J.C. Giddings, A new method for the prediction of binary gas-phase diffusion coefficients, *Industrial & Engineering Chemistry* 58 (5) (1966) 19–27.
- [59] M. Brown, S. Primdahl, M. Mogensen, Structure/performance relations for ni/yttria-stabilized zirconia anodes for solid oxide fuel cells, *Journal of the Electrochemical Society* 147 (2) (2000) 475–485.
- [60] L. Andreassi, G. Rubeo, S. Ubertini, P. Lunghi, R. Bove, Experimental and numerical analysis of a radial flow solid oxide fuel cell, *International Journal of Hydrogen Energy* 32 (17) (2007) 4559–4574.
- [61] J.W. Eaton, *GNU Octave Manual*, Network Theory Limited, 2002.
- [62] <http://www.octave.org>.